Thermal Energy Storage in PCM-Filled Boreholes

Evaluating the energy performance of a PCM in a borehole process, confined to the Dutch mainland, when varying the diameter of the borehole, the temperature or the mole fraction of PCM

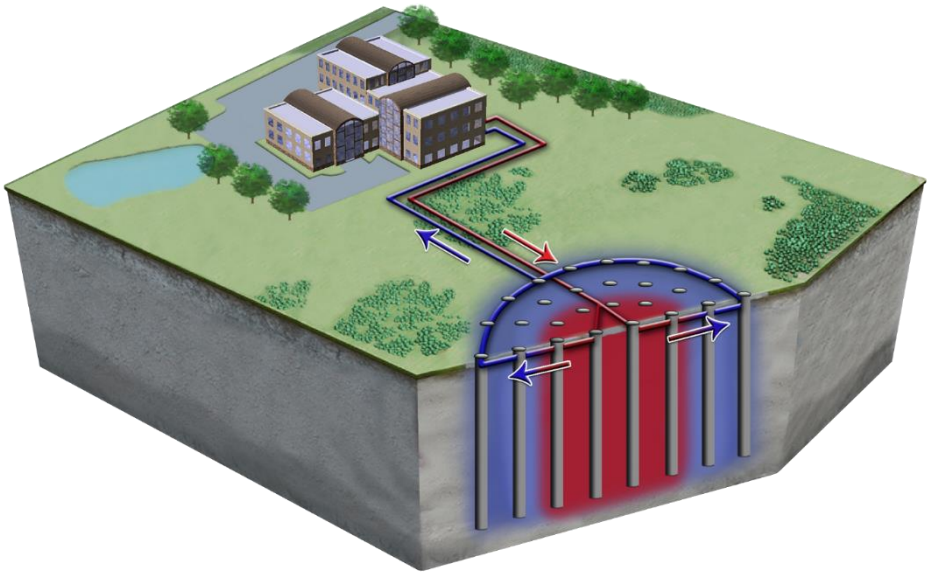

Source: (BTES | Underground Energy, 2019)

Minor Engineering for Large-Scale Energy Conversion and Storage

Design Project Renewables Based Energy Conversion and Storage (WB3595)

TU Delft

Students:
Teise Stellema (4763165)
Niels van Vliet (4952669)
Patrick Widdows (4720318)
Lucas Wiedenhoff (4952332)
Lars Wielinga (4719670)

Supervised by:
Dr.ir. J.M. Bloemendal
Dr.ir. J.W.R. Peeters

Abstract

As a consequence of the energy transition to renewable energy sources, energy storage technologies are required to address the intermittency of renewables. One such technology, borehole thermal energy storage (BTES), is a well-established technology and a promising option for the large-scale deployment that the energy transition will require. This is due to its long-life span and low capital costs. Its energy storage capacity and efficiency have significant room for improvement. Utilising phase-change materials within the borehole has been theorised to improve both these aspects significantly. This is due to the latent heat capacity of phase-change materials (PCM) and its ability to operate within the narrow temperature range typical of BTES systems. This work answers how the introduction of PCM materials improves a BTES system's performance and how to optimally implement PCM material into a BTES system. It does so by deriving and then using a numerical model, implemented in python, to simulate a BTES system's behaviour under a range of conditions and dimensions. The addition of PCM to the BTES system yielded a significant increase in efficiency. When the soil was chosen as sand, a BTES system without PCM was able to recover 38.98% of the heat stored. In the same conditions, introducing PCM resulted in a recovery of 66.73% of the heat stored. The maximum efficiency (71.93%) was achieved by the usage of a PCM “RT35hc” for the first meter of the borehole, heating the borehole at 55 degrees Celsius and cooling the borehole at 1 degree Celsius.

Table of Contents

Nomenclature

Symbol	Definition
A	Area [m^2]
c_p	Specific heat capacity [J/kg·K]
dL	Length step [m]
dt	Time step [s]
Fo	Mesh fourier number [-]
h	Height borehole [m]
k	Thermal conductivity [W/m·K]
L_{tot}	Total radius [m]
l	Height borehole [m]
M	Mass [kg]
Q	Heat flow [W]
Q_{in}	Incoming heat transfer [J]
Q_{out}	Outcoming heat transfer [J]
q	Heat flux [W/m^2]
q_i	Heat flux at radial coordinate i [W/m^2]
R_{cen}	Radius U-pipe [m]
r	Radius [m]
r_i	Distance to radial coordinate i [m]
T	Temperature [°C]
T_c	Temperature cooling water [°C]
T_h	Temperature heating water [°C]
T^n_i	Temperature at time n and radial coordinate i [°C]
t_{end}	Total running time [s]
t	Time [s]
U	Internal energy [J]
V	Volume [m^3]
ρ	Density [kg/m^3]
η	Efficiency [-]
α	Thermal diffusivity [m^2/s]

1. Introduction

The last decades there has been an enormous increase in energy demand. Until now this energy demand has been fulfilled with carbon-based fuels which emit large amounts of CO_2. In order to reduce the amount of carbon dioxide in the atmosphere, a global energy transition to renewable energy sources is required (Rogelj et al. 634). The abundant renewable energy sources such as wind and solar are intermittent, which causes a mismatch in supply and demand. In order to make renewable energy sources viable for continuous energy supply, current energy storage methods must be optimised, and new methods must be . One such method of energy storage, specifically in the form of heat, is borehole thermal energy storage or BTES for short.Thermal energy storage in boreholes is based on vertical 'U-pipe' heat exchangers installed underground (Figure 1), which enables the transfer of thermal energy between the pipe and the ground layers (sand, clay and rock). Various substances can be surrounding the U-pipe to aid the transfer of thermal energy. An example of such substances are phase change materials or 'PCMs', such as water, polyglycols, salts and paraffins. These materials are of particular interest due to their ability to store large amounts of heat during their phase transition in other words latent heat capacity. Another point of interest is the application of PCM boreholes in residence areas, as the small thermal diffusivity of such boreholes allow them to be built closer together, as is desirable for a residential areaBTES systems can be employed when there's a periodic mismatch in supply and demand for energy. Further research is necessary to assess these PCM BTES systems, especially when comparing their performance with those of traditional BTES systems to increase their already large potential.to increase their already large potential.

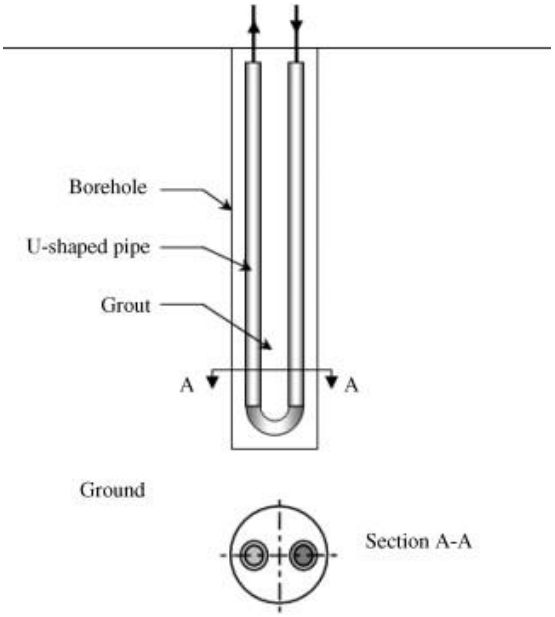

Figure 1: U-pipe borehole. (Sharqawy, Mokheimer, & Badr, 2009, p. 274)

This report answers the following research question: *In what ways does the energy performance of a phase change material (PCM) in a borehole process, confined to the Dutch mainland, change when varying the PCM, the molefraction of the PCM, the diameter of the borehole or the temperature of heating and/or cooling?* This question will be answered by literature research, followed by the derivation and implementation of the obtained parameters into a numerical model of heat transfer in Python. In this analysis the energy performance of the system will be interpreted as the efficiency, so the thermal energy that is recovered from the system divided by the thermal energy that enters the system.

This report has the following structure. First, the results of the literature study are shown. Secondly, the methodology is explained. Furthermore, the numerical method is explained as well as is its implementation in Python. The last part of the methodology consists of an overview of the simulations. Thirdly, the results are shown and discussed, followed by the conclusion and the evaluation. Finally, recommendations are given for further research.

2. Literature study

In order to perform a coherent literature study, relevant scientific research was individually pursued and subsequently summarized in short literary reviews. The reviews will each be presented, and relevant conclusions and data are then discussed. The following will summarize the discussions and separate reviews to display the formulation of the research question.

The parameters that are responsible for fluctuation in the borehole's energy performance were discussed and resulted in 3 independent variables: the borehole diameter, PCM concentration and operating temperature of the BTES system. Establishing a proper baseline to ensure a reliable trend among the independent variables was necessary, thus construction of a network of controlled variables was completed. The necessity of controlled variables opted into a thorough ground analysis reinforced by identifying the dominant heat transfer mechanism, in this case conduction.

The ground analysis was confined to the Dutch mainland and yielded two relevant ground types: river clay and sand. Each ground type comprised of three layers; however, the layers were deemed insignificant to the scope of this research due to past sources regarding them redundant in their respective ground analyses (Jaime van Trikt & Hansjorg Ahrens, Naturalis) (Indra Noer Hamdhan and Barry G. Clarke,2010). The thermal conductivities for river clay and sand had large ranges, 0.25 - 1.52 (W/m*K) and 0.15 - 3 (W/m*K) respectively. Sand has a higher conductivity which implied it would have a greater effect on the heat loss of the borehole. Therefore, to maintain the realistic integrity of the research sand was selected as the ground type. Presumably, clay would benefit the performance of the borehole more so than sand.

Moreover, various borehole diameters were examined:

- 152 mm (Welsch et al., 2016, p. 1858)
- 155 mm (Stene, J., 19 May 2008)
- 114 mm (Lanini et al., 2014, p. 399)
- 228 mm (Nakevska et al., 2014, p. 254)
- 120 mm (Zhang et al., 2016, p. 1186)
- 100 - 150 mm (Skarphagen et al., 2019, p. 17)

Huang et al. (2014), had extensively investigated the ideal design parameters of a borehole. Ranges of design parameters were established based on previous engineering projects. These ranges resulted in an ideal diameter for a borehole of 2*60 = 120 mm when combined with a borehole depth of 126 m.

The diameters which were mentioned in the other research, vary between 100 and 155 mm (apart from outlier 228 mm). Therefore, we can conclude that 100-120 mm are suitable diameters for a borehole. Note these boreholes are traditional BTES systems where the borehole's primary function is as a heat exchanger. In this research the boreholes are also used as thermal storage.

To examine the PCM concentration, a paper written by Pasupathy & Velraj (2008) was consulted. It theoretically concluded that a greater quantity of PCM would cause a greater storage capacity of heat, due to a main principle in thermodynamics. This principle states that the amount of energy released or absorbed during a phase transition is larger than the energy stored as sensible heat.

In addition, the selection of the specific PCMs was based on the readily available data of the organization Rubitherm (Appendix 5) and the compatibility of the PCMs with corresponding operating temperature of the borehole (1-70^{o}C). As the selection was made predominantly between organic PCMs, toxicity and corrosivity did not form a problem. For obvious reasons the PCMs with the highest

theoretical heat storage capacity was used, while still satisfying the previously mentioned conditions. These conditions yielded RT35hc and RT44hc which are both paraffin waxes, as suitable options.

Finally, a higher temperature gives rise to a larger thermal radius. Due to this larger radius more energy can be stored, however it has a greater incentive to dissipate to the environment as the area significantly increases. Numerical analysis should therefore look for a compromise in the amount of energy stored and acceptable losses.

3. Methodology

The goal of this paper is to characterise the performance of a borehole thermal energy storage system while varying several variables. A numerical model will be used to answer this research question. Firstly, all assumptions made are presented in a general overview. Secondly, the numerical model is derived. This is done by first deriving a linear numerical model for heat flow and then translating this to a radial model. This order allows the focus to first be solely on formulating and discretising the heat flow model. The focus then shifts entirely to the consequences of a radial model and numerical element. This is deemed clearer than solving both aspects simultaneously. Thirdly, a stability analysis for the length- and timestep is shown, the numerical model is validated by comparing it to known analytical solutions and then the model's implementation in python is explained. Lastly, the simulations are shown.

3.1 Model assumptions

The following assumptions are made for the analytic model used in this research:

1. The heat flows are confined to one direction. In the case of the Cartesian vector space, as seen in figure 6, the x-axis. In case of the radial vector space, the r-axis. All other axes are assumed to be uniform and constant in temperature, thus the heat flow is zero.
2. Utilization of a step function (seen in the left graph of figure 2) for a phase change trajectory is sufficient. Due to the small Temperature window of this phase changing trajectory (seen in right graph of figure 2) the assumption does not introduce a relevant error.

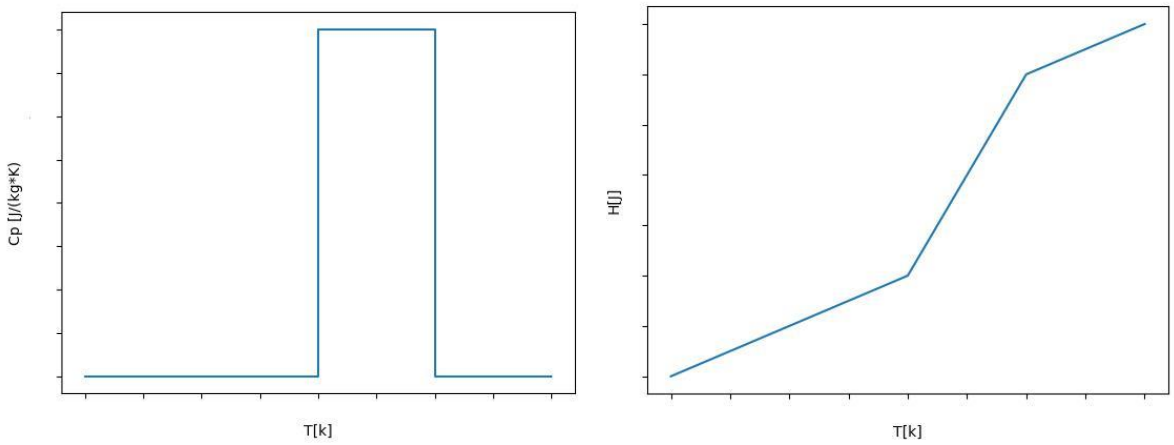

Figure 2: Phase change trajectory.

3. Ambient air temperature does not affect borehole temperature.
4. In case of mixing, the PCM and sand are a homogeneous mixture, in other words chemical potential is 0.

5. The temperature of the water does not change when it gets to the lower parts of the borehole and does not cool the borehole on its way back to the surface (figure 3).

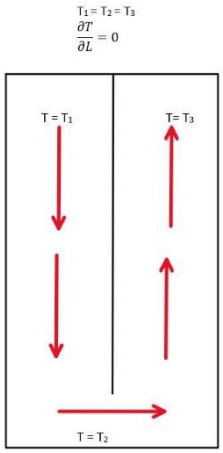

Figure 3: No temperature change occurs during water transport through the borehole.

6. A cycle of a year is split in cooling and a heating period each consists of 6 months in which the heating and cooling temperatures are consistent. Meaning the system preheats the water when heating and precools the water when it recovers the heat. (figure 4)

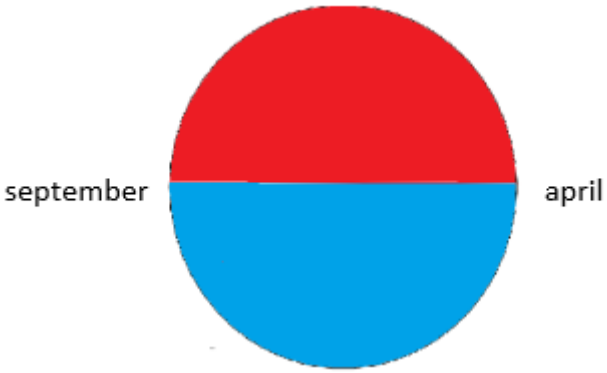

Figure 4: Heating and cooling distribution during a cycle.

7. For a single cycle, the temperature gradient becomes negligible after 20 meters. For the 30-cycle scenario, this distance increases to 40 meters. Thus, the borehole does not lose significant heat to the surrounding area shown in figure 5.

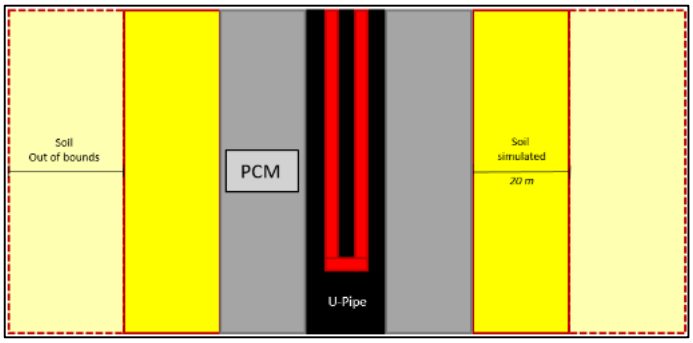

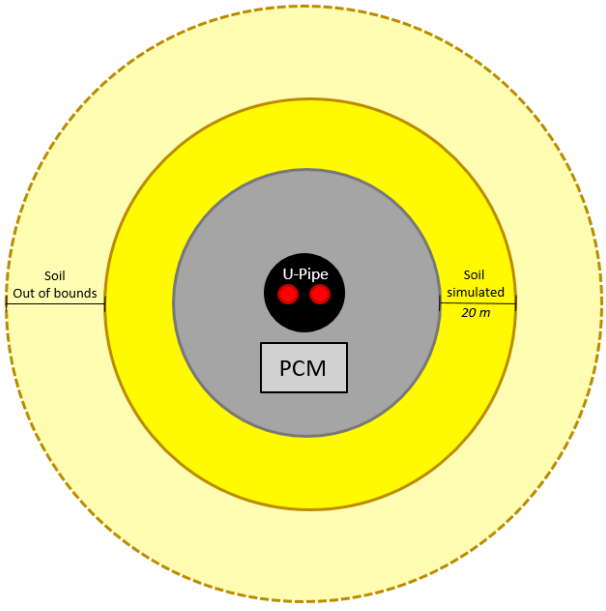

Figure 5: Thermal radius borehole.

3.2 General model theory

A numerical model will be used to simulate the response of the borehole when the work fluid flows through the borehole, represented by a temperature gradient. The borehole can be described by a cylindrical volume of length L and radius r.
Following the first rule of thermodynamics the energy balance for the borehole can be formulated. If we assume there is no work done and that there are no changes in kinetic or potential energy, we conclude that any heat transported to the system is stored in the form of internal energy. Substituting the expression for internal energy and the heat flux we arrive at the following equation.

$$dU = Q \rightarrow c_p \, V \, \rho \, dT = \, q_{in} \, A - q_{out} \, A \qquad [1]$$

The heat flux in this equation can in turn be substituted according to Fourier's law. For the purposes of deriving a numerical model, the first step is considered to be formulating a model for 1 dimensional heat transfer in a classic Cartesian axes system. As a BTES system is comprised of a cylinder, it follows that translating the initial model to a circular axes system is advantageous. After this the model could either be made to calculate over the angle of the circle or going from a circle to a cylinder. As the only real difference over the angle is a minor temperature gradient due to the U-pipe's shape it is not deemed worth the calculation time. Calculating over the length of the borehole using a cylindrical system could provide relevant data as it would enable the model to differentiate between different soils at different heights. Neither of these hypothetical models were deemed necessary as a 1-D radial model is sufficient for the scope of this paper

3.3 Formulating the 1-dimensional linear model

Taking a slab of length L that is adiabatic over the edges parallel to the x-axis and has boundary temperatures T_0 and T_1 at the y-parallel sides as depicted in figure 6.

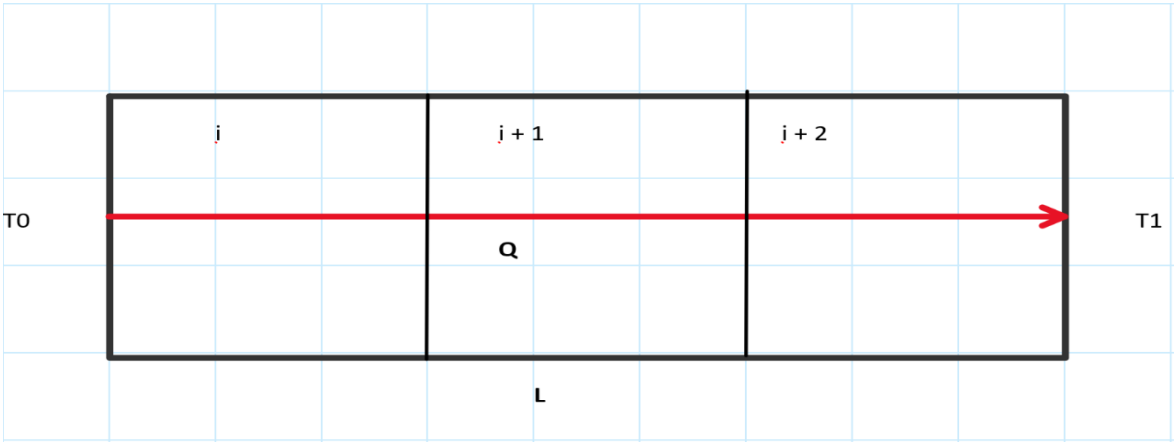

Figure 6: Slab 1-dimensional model.

Dividing this slab into several grid points i, each with a control volume around it of length *dL*. As heat conducts from T_0 to T_1, each subdivided slab will have heat flow in and out in this same direction. Using equation 1 we formulate:

$$c_p\, A\, dx\, \rho\, dT = A\left(q_{i-\frac{1}{2}} - q_{i+\frac{1}{2}}\right) => \; c_p\, dx\, \rho\, dT = \; q_{i-\frac{1}{2}} - q_{i+\frac{1}{2}} \qquad [2]$$

Which essentially states that the internal energy change of the element *i* is the net heat flow over its borders.

We can then quantify the heat flow using Fourier's law to the following approximation:

$$q_{i-\frac{1}{2}} = \; -k\frac{\partial T}{\partial x} \; \approx \; -k \; \frac{T_i - \; T_{i-1}}{\Delta x} \qquad [3]$$

This is done for the heat flow over the left boundary and can done in the same form for the right boundary. Substituting these expressions into equation 2 gives the following discretised form for heat diffusion:

$$c_p\, dx\, \rho\, dT = \; -k\left(\frac{T_i - \; T_{i-1}}{\Delta x} - \frac{T_{i+1} - \; T_i}{\Delta x}\right) => \Delta T = \; -\propto \; (\frac{-T_{i+1} \; + \; 2T_i \; - \; T_{i-1}}{\Delta x^2}) \qquad [4]$$

The final step following the formulation of equation 4 is to discretise for time as well as length to build the numerical model. This can be done by rewriting the *ΔT* term in the following way:

$$dT = \frac{\partial T}{\partial t} \; \approx \; \frac{T_i^{n+1} - \; T_i^n}{\Delta t} \qquad [5]$$

This expression can be substituted into equation 4 giving an expression for the temperature of element *i*. The choice is made to explicitly time integrate by right hand side evaluating equation 4. With this substitution and evaluation, we arrive at an expression for T_i^{n+1}, the temperature of element *i* at timestep *n + 1*, fully expressed in temperatures of the previous time step, given as equation 6.

$$T_i^{n+1} = \; T_i^n + \propto \Delta t * (\frac{T_{i+1}^n \; - \; 2T_i^n \; + \; T_{i-1}^n}{\Delta x^2}) \qquad [6]$$

3.4 Formulating the 1-dimensional radial model

While the linear model provides a good foundation there is an important divergence from it regarding the temperature behaviour in a borehole. When a slab of length *L* is divided into $2\pi r$ amount of slabs each slab has the same surface area. When dividing a borehole into circular elements extending from the centre the contact surface between each circle is defined as equation 7 where the radius *r* is expanding between each circle. This effectively means that while the heat flux *q* behaves similarly to the linear case, dependent solely on the material and the temperature gradient, as the area *A* increases as shown in equation 7 the heat flow *Q* behaves differently.

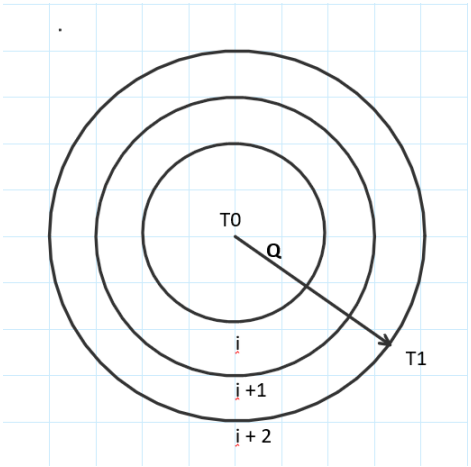

Figure 7: Display radial model.

$$A = \left(r \mp \frac{1}{2}\, dr\right) 2\pi\, h \qquad [7]$$

Recalling equation 1, the deviation from the linear case is both in the expression of the volume and the expression of the area over which heat is transported. The expression for the area of heat flow is simplest as this is the surface area of the cylinder with radius *r* defined as seen in equation 7.

for the expression of the volume of element i the following equation is used:

$$\pi\, (r_2^2 - r_1^2)\, l \qquad [8]$$

Where *l* is the height of the borehole and r_2 and r_1 are the outer and inner radius of the circle element respectively. Where the linear model divided into slabs of length Δl this model divides into circle elements of width Δr. Realising that the outer radius of element i is the inner radius plus Δr and substituting into the expression for volume:

$$V = \pi l\, ((r + \Delta r)^2 - r^2) = \pi l\, (2r\Delta r + \Delta r^2) \qquad [9]$$

This expression can be simplified with the knowledge that Δr by definition is a very small element, as denoted by delta. In comparison to this the r component of the expression is much larger as this denotes the radius *r*. From this the condition and accompanying simplification can be formulated that while $\Delta r \ll r$ then $V \approx \pi l * 2r\Delta r$. substituting these expressions for area and volume for the now radial element i into equation 1 produces the following formula

$$c_p\, \pi\, l\, 2r\Delta r\, \rho\, dT = q_{in}\, 2\, \pi\, r_{i-\frac{1}{2}}\, l - q_{out}\, 2\, \pi\, r_{i+\frac{1}{2}}\, l \qquad [10]$$

This simplifies to:

$$c_p\, r_i \Delta r\, \rho\, dT = q_{in}\, r_{i-\frac{1}{2}} - q_{out}\, r_{i+\frac{1}{2}} \qquad [11]$$

This equation can then be combined with Fourier's law for heat conduction similarly to the steps that were taken to formulate equations 3 & 4. As Fourier's law can be formulated for both a Cartesian and a radial coordinate system, both variants can be discretised in the same way as well. Replacing *Δx* with *Δr* in equation 3 and substituting this into equation 11 leads to the following expression:

$$c_p\, r_i \Delta r\, \rho\, dT = -k\, \frac{T_i - T_{i-1}}{\Delta r}\, r_{i-\frac{1}{2}} - \left(-k\, \frac{T_{i+1} - T_i}{\Delta r}\, r_{i+\frac{1}{2}}\right) \quad [12]$$

which simplifies to:

$$r_i \Delta r\, dT = -\propto \left(\frac{T_i - T_{i-1}}{\Delta r}\, r_{i-\frac{1}{2}} - \frac{T_{i+1} - T_i}{\Delta r}\, r_{i+\frac{1}{2}}\right) \quad [13]$$

Finally, substituting the radius components of the equation the following equation is found:

$$dT = -\frac{\propto}{r}\left(\frac{(T_i - T_{i-1})\left(r - \frac{1}{2}\Delta r\right) - (T_{i+1} - T_i)\left(r + \frac{1}{2}\Delta r\right)}{\Delta r^2}\right) \quad [14]$$

Which is recognised as the radial variant of equation 4 and can be called the discretised formula for radial heat diffusion. This equation gives the temperature change of the hollow cylinder element i with a radius to the centre of *r* and a width Δr. Discretising this equation over time by substituting equation 5 into equation 14 and right-hand side evaluating the following equation the following explicit numerical model is found:

$$T_i^{n+1} = T_i^n - \frac{\propto \Delta t}{r}\left(\frac{(T_i^n - T_{i-1}^n)\left(r - \frac{1}{2}\Delta r\right) - (T_{i+1}^n - T_i^n)\left(r + \frac{1}{2}\Delta r\right)}{\Delta r^2}\right) \quad [15]$$

3.5 Model implementation

The 1-dimensional radial model was chosen and comes with several stability and accuracy conditions.

3.5.1 Stability

When reviewing equation 15, the governing equation of the radial heat transfer model was formulated using an assumption in the derivation of the volume of the circle elements. The assumption, $\Delta r \ll r$, will cause an inaccuracy in the model if it's not abided by. It should be noted however that this assumption will not cause instability.

In addition to the restrictions given by the made assumptions, any numerical model should also be investigated for stability. This can be done by substituting mesh Fourier numbers into equation 15 and then investigating which parts of the formula can cause divergent oscillations. Following the derivation in appendix 4**,** the stability condition was found to be that the coefficient for T_i^n cannot be negative. As the coefficient was found to be: $(1 - 2Fo)$ with $Fo = \frac{\propto \Delta t}{\Delta r^2}$

This means the stability condition can be defined as $\Delta t \leq \frac{\Delta r^2}{2\propto}$.

The alpha component of the stability condition means that the type of material being simulated affects the restrictiveness of the stability condition. This means that when determining the stability condition the most restrictive material determines the overall time step.

3.5.2 Validation

It is valuable to validate the numerical model as much as possible as to increase the likelihood of accurate results. First is the similar shape argument. If one would analytically convert a Cartesian heat conduction equation to a radial one that conversion would use equation 16 (Mills & Coimbra, 2015, pp. 65–73).

$$\rho\, c_p \frac{\partial T}{\partial t} = \frac{k}{r} \frac{\partial}{\partial r}\left(r \frac{\partial T}{\partial r}\right) \qquad [16]$$

If we compare this general shape to the shape of equation 14 we see a very similarly shaped equation. The division over Δr squared in equation 15 mirrors the double partial derivative over *r* in equation 16. Both equations 15 and 16 also divide over *r*. these similarities give credibility to equation 15.

The strongest validation possible would be to show that the numerical model yields an approximately equal result to an analytical solution. While solving the general heat transfer analytically is not possible, solving analytically for steady-state is possible. This means that if the numerical solution's steady-state is the same as the steady-state found by the analytical solution that would strongly indicate that the model is credible.

(Mills & Coimbra, 2015, pp. 65–73) The analytical solution for steady-state conduction through a cylinder is:

$$\frac{T_1 - T}{T_1 - T_2} = \frac{\ln\left(\frac{r}{r_1}\right)}{\ln\left(\frac{r_2}{r_1}\right)} \qquad [17]$$

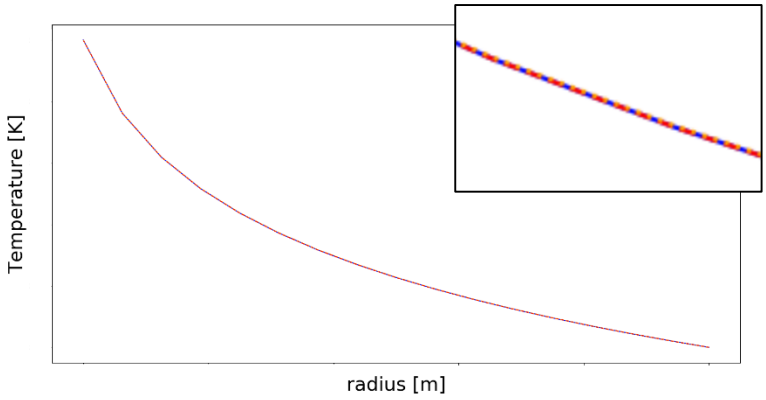

Figure 8: Plot analytical solution.

This formula can easily be plotted when taking the boundaries 1 (r_1) and 2 (r_2) as the known radius and temperature of the U-pipe that heats the borehole for boundary 1 and taking the soil as boundary 2. In order for the model to approach steady-state the quickest it was ran without any PCM, as the thermal diffusivity of the PCM is significantly lower than that of sand. In figure 8 three lines have been plotted on a temperature and radius scale of which the numerical value has no further significance. The analytical solution is given by the yellow line, the red and blue lines are the numerical solution at the final time and at 10 seconds before to show that not only does it overlap with the analytical solution, it does so consistently.

3.5.3 Grid independency study

The runtime is based upon the number of calculations that need to be done in order to numerically calculate the temperature in the radial element at all timesteps as well as all the length steps. Obviously increasing *dt* and *dL* will decrease the runtime. Unfortunately, this makes the method unreasonably inaccurate. The time step can be based upon the length step with the stability condition.

Using trial and error the efficiency was calculated for various length steps, for which the maximal time step was calculated with the stability condition. The formula of the stability condition shows that the timestep decreases very rapidly when decreasing the length step. Therefore, the running time of the model will increase exponentially with a smaller length step. The efficiency of a sand and a PCM borehole was calculated, as well as the difference between the two and the ratio. This ratio is mainly important for the research as it compares two different cases. The results are shown in table 2.

Table 1: Efficiency differences and ratio.

dL [m]	η Sand	η 0.5 m PCM	Difference	Ratio
0.5	0.3052	0.404	0.0990	0.7550
0.2	0.2979	0.503	0.2048	0.5925
0.1	0.2953	0.535	0.2400	0.5516
0.05	0.2953	0.546	0.2508	0.5408
0.02	0.2958	0.550	0.2543	0.5377

When dL is decreased, the efficiency approaches the actual efficiency of the modelled borehole. When further decreasing the length step after *dL* = 0.05 m the efficiency only changes very slightly, as well as the fact that the ratios for *dL* = 0.05 m and *dL* = 0.02 m between the two boreholes (sand and 0.5 m PCM) have a difference of just 0.58 %. This difference has been decided as an acceptable error; thus *dL* = 0.05 m was finally chosen as length step. This required a maximum time step, according to the stability condition, equal to 1223 s for a model with sand. The time step was then decided as *dt* = 120 s, a tenth of the required time step, in order to be on the conservative side of the condition. Of course,

it is debatable whether the accuracy is sufficient, but in the research calculations the 0.58% was a lot smaller than the actual differences in the comparisons made, so therefore it was accepted.

3.5.4 Code

The python coding language was selected for implementing formula 15. The first step is to define all necessary variables, starting with the operating temperatures and the relevant dimensions of the borehole. As the model cannot distinguish over its height this variable's only effect is scaling the value of the heat in- and outflows.

The second step is modelling the borehole material. A major assumption in the model is that the phase change can be simulated by increasing the heat capacity within the temperature range where the PCM would melt. This means that the heat capacity is effectively shaped like a block curve as shown in the figure 2 under assumption 2.

Implementing the change in PCM concentration in the borehole is achieved by denoting the respective mass fractions. The main effect of altering the mass fractions, is the change in specific heat capacity. Utilizing the 'Rule of mixtures', equation 18, a relative specific heat capacity for the different PCM concentrations is evaluated ("Rule of Mixtures Calculator for Heat Capacity", 2017).

$$C_p(mixture) = C_{p1}\frac{M_1}{M_1 + M_2} + C_{p2}\frac{M_2}{M_1 + M_2} \quad [18]$$

Furthermore, the density of PCM is altered by the phase change process. In other words, when the PCMs are in the liquid phase the density varies from their respective solid phase densities. This phenomenon was implemented in the code using a simple 'if statement' resulting in a step function on the phase boundary temperatures. This can be seen in appendix 1 python code, line 39.

The model then uses equation 15 to simulate the temperature change over time and radius. It was assumed that the heating and cooling periods of the borehole can be seen annually as 6 months of heating and 6 months of cooling. Lines 123 – 151 of the code, found in appendix 1, show how the model divides the given time in seconds over the given cycles and then separates those cycles in 50/50 segments.

The final part of the implementation revolves around translating the temperature response of the system into a value of heat energy. As the research question focusses on the energy efficiency, the energy stored and the energy recovered from the borehole during operation need to be extrapolated from the temperature data. We define the heat flow as the amount of Joule exchanged between the u-pipe and the borehole. The efficiency η is defined as the ratio of heat recovered from the borehole over the heat supplied to the borehole.

Two methods were considered to calculate the energy flow. The first theory was to calculate the area under the graph after finishing the heating process and again after the cooling process. These integrals would respectively be all the energy present in the borehole after heating and all the energy left after extraction. All the energy that is present after heating is the energy input. The energy output could be found by subtracting the energy remnant from the energy input. As all the energy inputted minus the energy left after extraction simply is the energy extracted. This method was effective for one cycle but proved difficult to implement for multiple consecutive cycles. As an alternative method was available this implementation was not finalised.

The alternative method was theorised based on the definition of control volumes. As illustrated in figure 9, the heat flow into the borehole and the heat recovered from the borehole are both done through the contact with the U-pipe. The idea that follows is that any heat conducted to or from the borehole must be conducted through the very first element i = 1. As the heat flow is the contact area times the heat flux, using Fourier an equation for heat flow can be formulated and is implemented on lines 71 – 75.

$$Q = q\,A = -k\frac{T_1 - T_0}{\Delta r}\,2\pi h r_1 = 2\pi\,h\,k\,r_1\,\frac{T_0 - T_1}{\Delta r} \qquad [19]$$

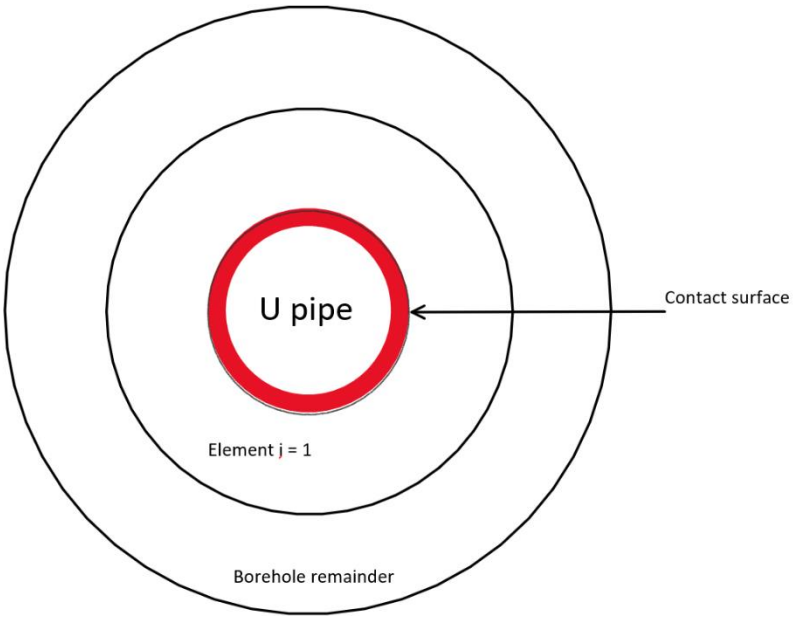

Figure 9: Intersection borehole.

3.6 Simulations

To answer the research question, the main variables; PCM or sand, mole fraction, radius and temperature will be tested. To see if the influence of these variables differs after a certain amount of time, there will also be simulations with a distinct number of cycles. The variables thus are:

- PCM (RT44hc/RT35hc) or no PCM (sand)
- Radius (PCM)
- Mole fraction
- Temperatures

3.6.1 PCM

Two different PCM's were selected, namely, RT35hc and RT44hc. Furthermore, the simulation was run with sand, however its efficiency was expected to be much lower than that of the PCM boreholes. The selection of the PCM's has been done in the Literature Study. The physical properties can be found in the appendix 5A:RT44hc and 5B:RT35hc; PCM mixtures and specific heat capacities. The expectation is that RT35hc will be more efficient because of its slightly lower melting area. To ensure this trend continues the RT44hc will also be run for multiple cycles. These long-term simulations apply to simulation 13 and 22 as can be seen in table 2 together with the one cycle simulations. The simulation numbers refer to the simulation matrix which can be found in appendix 2.

Table 2: PCM simulations.

Simulation	**PCM**	**L_{Total} [m]**	**Radius [m]**	**Mole fraction**	**Cycles**	**T_h [T]**	**T_c [T]**
1	Sand	20	0	1	1	60+273	6+273
2	RT35hc	20	1		1		
3	RT44hc	20	1		1		
13	RT35hc	40	1		30		
21	Sand sand	40	0		30		
22	RT44hc	40	1		30		

3.6.2 Radius

To determine the optimum amount of PCM to reach an efficiency as large as possible, the radius of the borehole, fully filled with PCM, is varied. As could be read in the literature study, the mean value of a borehole radius is about 0,1 to 0,15 meters. The expectation is that, when filled with PCM, the diameter needs to be larger. For this reason, the simulations will be run for the cases in which the radius is 0,1; 0,25; 0,5; 1; 2,5 and 5 meters. In earlier simulations, only the first 4 options were simulated. From those simulations it could be concluded that the efficiency was still increasing, so to track down the optimum in efficiency according to the radius, 2,5 and 5 meters were added. Firstly, the varying radius is tested for one cycle. Secondly, the boreholes are being tested for 30 cycles. Since, the heat reaches further in this case, the total length is now set to 40 meters. All radius compared simulations were noted in table 3.

Table 3: Radius simulations.

Simulation	**PCM**	**L_{Total} [m]**	**Radius [m]**	**Mole fraction**	**Cycles**	**T_h [°C]**	**T_c [°C]**
2	RT35hc	20	1	1	1	60	6
4			0.1				
5			0.25				
6			0.5				
7			2.5				
8			5				
13		40	1		30		
23			0.1				
24			0.25				
25			0.5				
26			2.5				
27			5				

3.6.3 Mole fraction

After fulfilling the varying diameters containing only PCM, the next interesting question is if it is really a need to totally fill the borehole PCM. Maybe a high efficiency is reached as well with a smaller mole fraction. For this reason, the following fractions will be tested: 0.2; 0.4; 0.6; 0.8 and 1 as can be seen in table 4. PCM is an expensive material, so any decrease of mole fraction without big losses in efficiency would be useful.

Table 4: Molefraction simulations.

Simulation	**PCM**	**L_{Total} [m]**	**Radius [m]**	**Molefraction**	**Cycles**	**T_h [°C]**	**T_c [°C]**
3	RT35hc	20	1	1	1	60	6
9				0.2			
10				0.4			
11				0.6			
12				0.8			

3.6.4 Temperatures

The initial cold and hot water temperatures have been respectively set to the realistic values of 6 and 60 degrees Celsius. These values are selected based on the maximum working temperature and the melting area of the chosen PCM materials. However, there is still some space to vary. To find the best combination, the following temperatures besides the initial values will be compared. These temperatures are displayed in Table 5. The first value refers to the heating temperature and the second to the cooling temperature, both in degrees Celsius. Note assumption 6.

Table 5: Temperature simulations.

Simulation	**PCM**	**L_{Total} [m]**	**Radius [m]**	**Molefraction**	**Cycles**	**T_h [°C]**	**T_c [°C]**
2	RT35hc	20	1	1	1	60	6
13		40			30	60	6
14		20			1	50	6
15						70	6
16						60	10
17						60	2
18						65	11
19						55	1
27		40			30	50	6
28						70	6
29						60	10
30						60	2
31						65	11

4. Results

Firstly, the raw data is displayed as graphs of the temperature in the borehole represented in a 1-dimensional manner over time for various simulations. This is mainly to illustrate the behaviour of the borehole. Secondly, the processed data of the simulations performed are given. Here the efficiencies and heat flows are analysed.

4.1 Raw data

The figures 10 to 15 give 10 instances in a cycle, given in days (noted in the legend), since heating was initiated. With the y-axis given in Kelvin and the x-axis given in meters. The first pair (figure 10,11) is used as the baseline for comparison, the second pair (figure 12,13) was the most efficient simulation and the last pair (figure 14,15) was the least efficient. The raw data of the heat flow and efficiencies can be found in appendix 2.

Note that the single cycles figures (figures 10,12,14) are shown for 20 meters (L_{tot}) and the thirty-cycle figure (figures 11,13,15) are shown over 40 meters (L_{tot}). What can be seen in figure 11,13 and 15 is that the later parts are hotter in case of the less efficient situations.

The interesting lines to follow in the figures are purple and light blue due to the fact that these lines represent the point at which the cycle changes from heating to cooling and cooling to heating respectively. What can be seen when followed chronologically is that heat steadily moves away from the u-pipe even when cooling and that this phenomenon is most apparent in figure 6 and least apparent in figure 4.

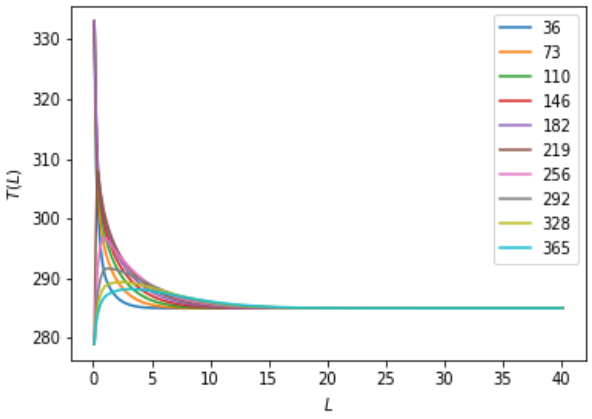

Figure 10: First cycle; sand, radius: 1 meter, mole fraction: 1, Th: 60°C, Tc: 6°C.

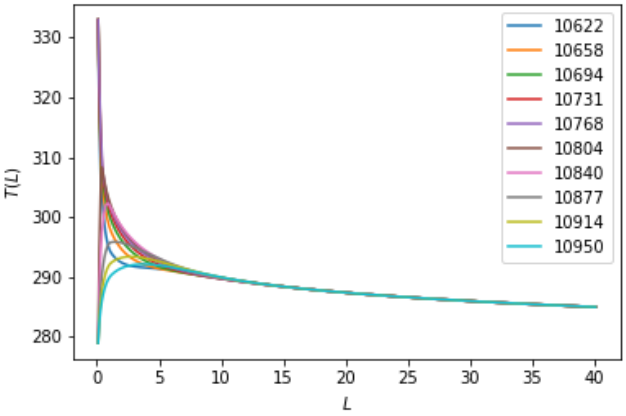

Figure 11: Last cycle; RT35hc, radius: 1 meter, mole fraction: 1, Th: 60°C, Tc: 6°C.

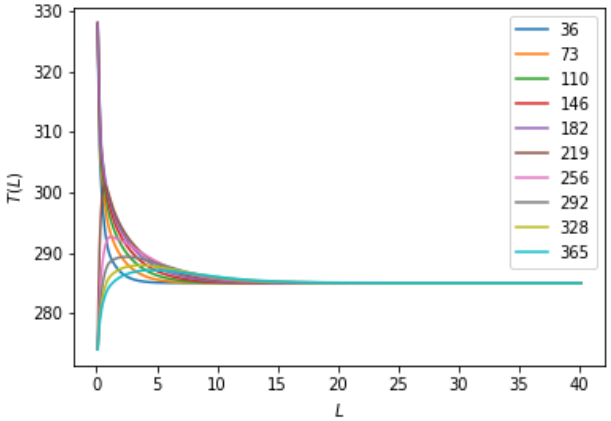

Figure 12: First cycle; RT35hc, radius: 1 meter, mole fraction: 1, Th: 55°C, Tc: 1°C.

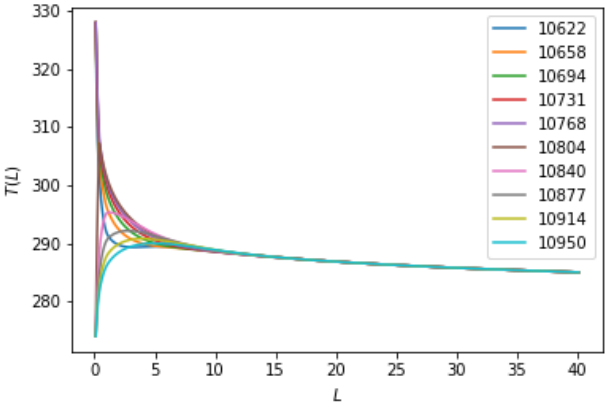

Figure 13: Last cycle; RT35hc, radius: 1 meter, mole fraction: 1, Th: 55°C, Tc: 1°C.

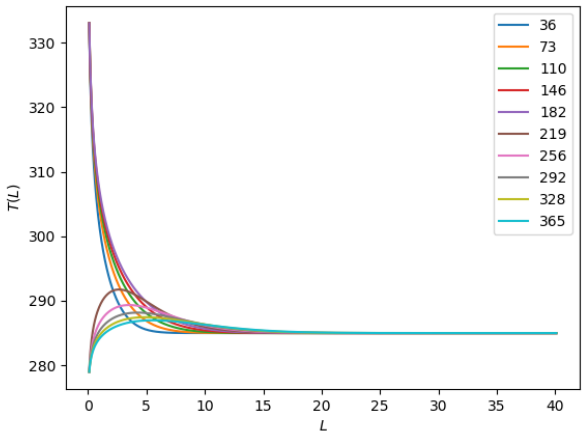

Figure 14: First cycle; sand, radius: 1 meter, mole fraction: 1, Th: 60°C, Tc: 6°C.

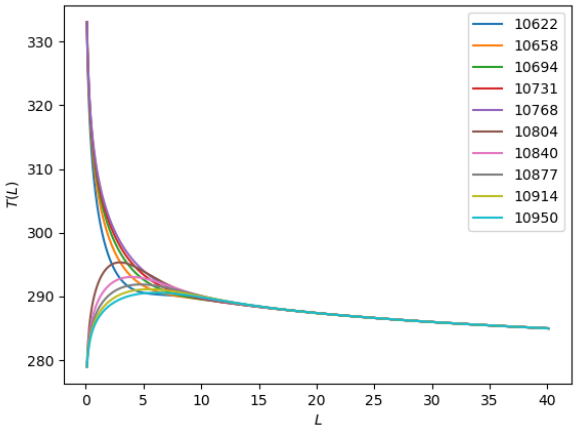

Figure 15: Last cycle; RT35hc, radius: 1 meter, mole fraction: 1, Th: 60°C, Tc: 6°C.

4.2 Processed data

Two types of data processing were performed. Firstly, a graph (x-axis independent variable, y-axis efficiency) was made for a single cycle which illustrates the different independent variables. Secondly, the thirty cycle graphs were made which show the efficiency of every run per independent variable. The accumulated efficiency up to that moment in time is represented by the uninterrupted line and the 'per cycle' data (per cycle efficiency) is represented with a dashed line, with the number of cycles on the x-axis. Consult appendix 3 for data on which the comparisons of the heat flows are based.

4.2.1 PCM

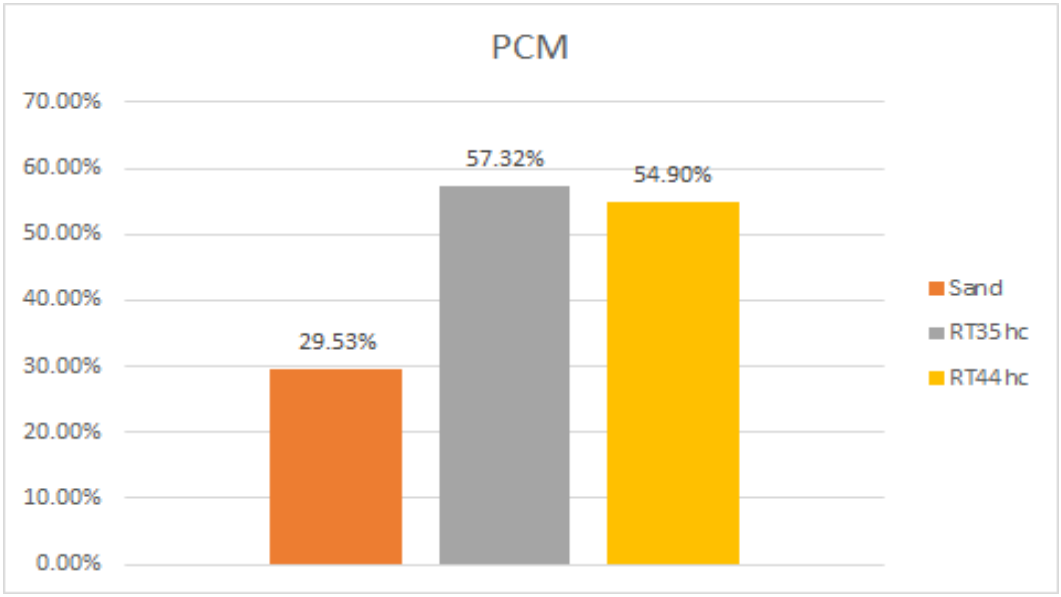

Figure 16: Comparison of the efficiency at varying PCM; 1 cycle.

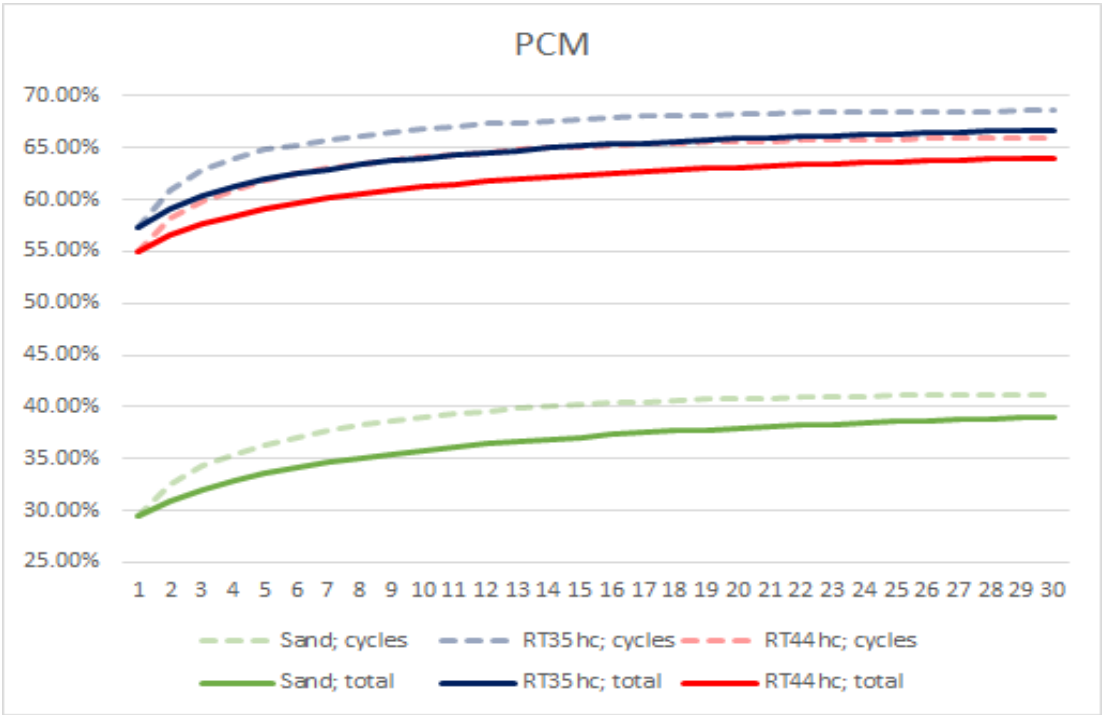

Figure 17: Comparison of the efficiency at varying PCM; 30 cycles.

Single cycle

In figure 12, the presence of PCM improves the efficiency significantly, yielding close to double the percentage of non PCM borehole. Another observation is that the PCM with lower melting point temperature has a higher efficiency despite a lower specific heat capacity, this means that having the latent heat for more points easily outweighs the loses from having less thermal capacity.

Thirty cycles

Figure 13 displays the continuation of the trend that can be seen in the first cycle. What can also be seen is that all the efficiencies increase with roughly ten percent over the thirty years.

Heat flow

The discrepancy in heat flow between sand and RT35hc is substantial and increases with 180% and 300% for the inflow and outflow respectively. The magnitude of the heat flows increases by 8% for inflow and 12% for outflow, when upgrading from RT44hc to RT35hc. These increases mean the thermal capacity of the borehole increases.

4.2.2 Molefraction

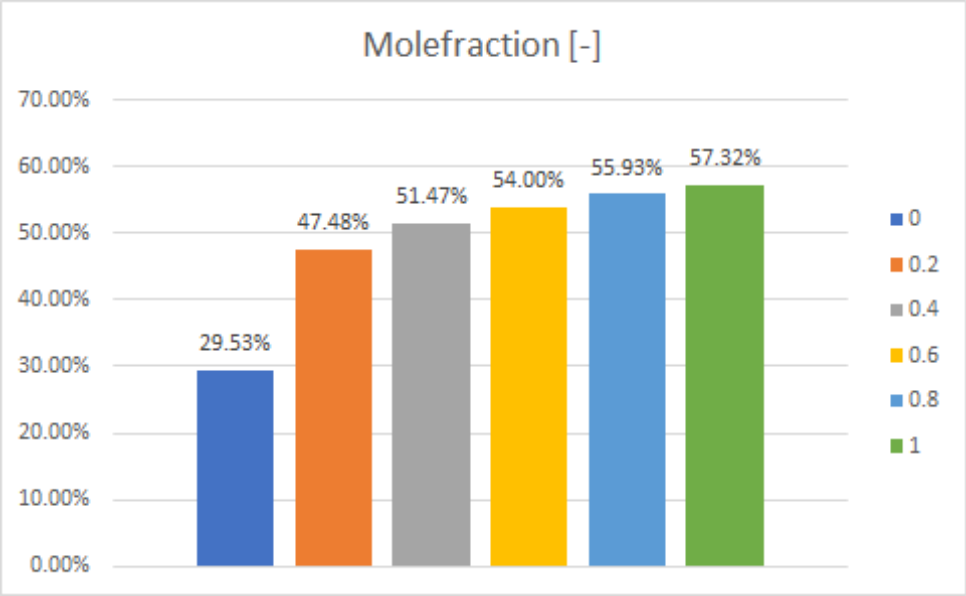

Figure 18: Comparison of the efficiency at varying molefractions; 1 cycle.

Single cycle

Figure 14 illustrates that when the PCM mole fraction increases, the efficiency increases alongside it. In addition, it is noticeable that it approaches a limit at a decreasing rate. This trend can be explained by the effect of PCM, which can be previously seen under PCM. By decreasing the mole fraction of PCM de effect of PCM decreasing.

Thirty cycles

Further inquiry towards the variation of the PCM mole fraction deemed unnecessary due to figure 14 displaying a clear pattern and would result in a mere continuation of this pattern when tested for thirty cycles.

4.2.3 Radius

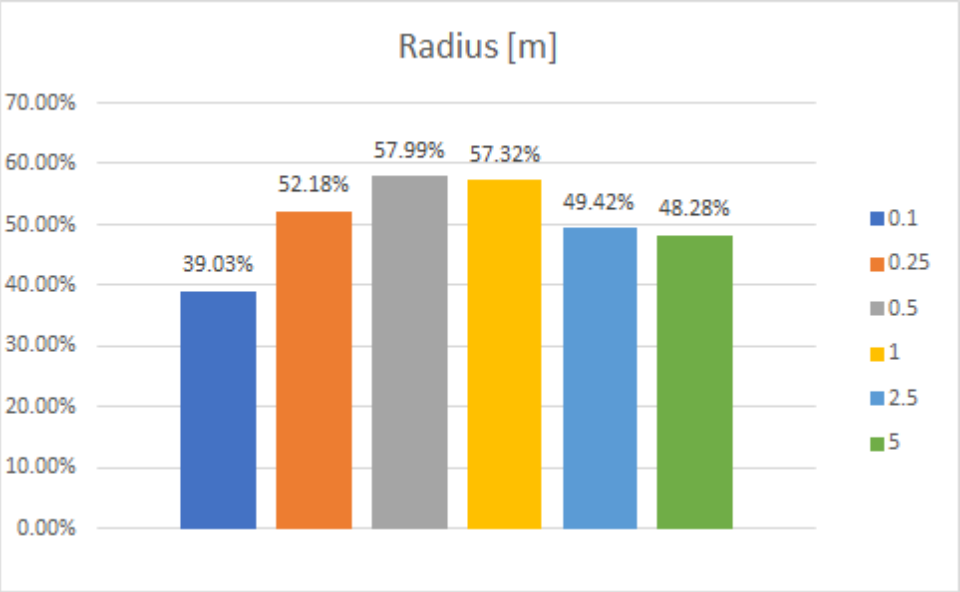

Figure 19: Comparison of the efficiency at varying Radii; 1 cycle.

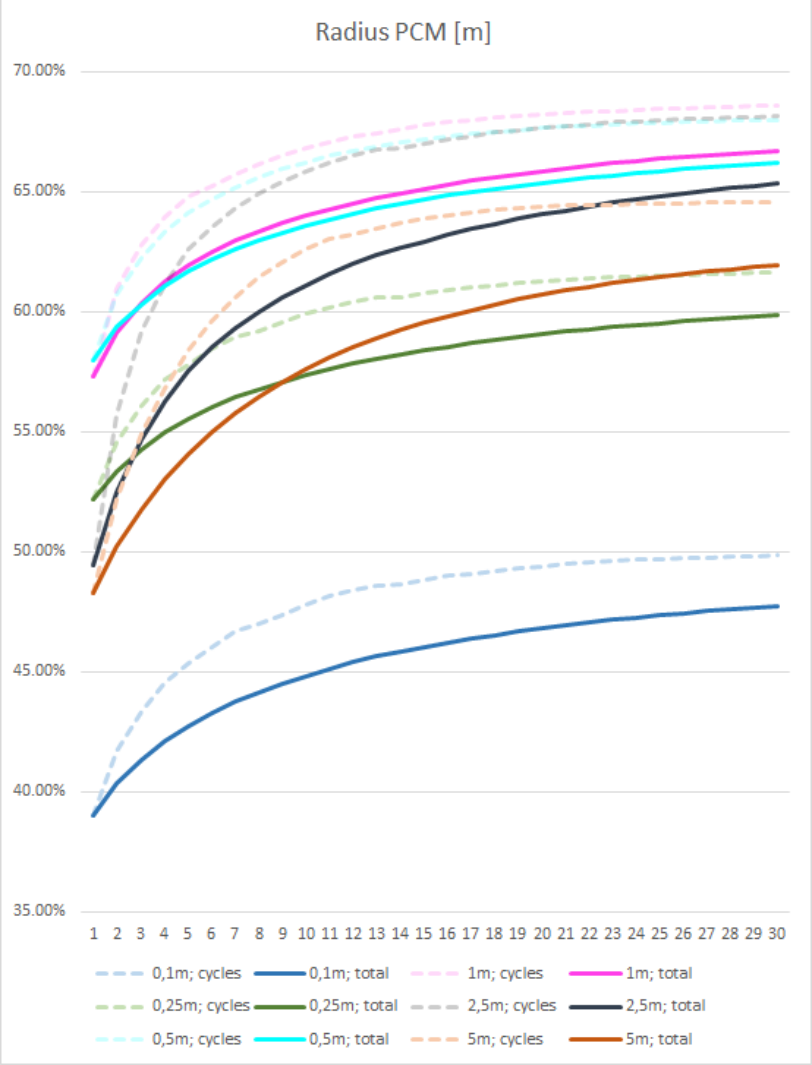

Figure 20: Comparison of the efficiency at varying radii; 30 cycles.

Single cycle

As can be seen in the Figure 15, the radius seems to have an optimum between 0.5 and 1 meter. Another observation is that it loses efficiency after 1 meter. However, it does not decrease significantly after 2.5 meters.

Thirty cycles

A few observations can be made in respect to radius in figure 20. Firstly, the larger the borehole, the slower the increase of efficiency. Another observation is that 0.5 metre to 1 metre still seems to be the optimal radii, where 1 meter overtakes the 0.5 meter over time. The last observation is that the bigger the borehole the longer the accumulated efficiency takes to approach the efficiency per cycle. The borehole with radius 0.25m initially has a higher efficiency, however it ends with a lower efficiency with respect to the boreholes with radii of 2.5m and 5m.

Heat flow

Increasing the radius from 0.25 meter to 0.1 meter gives an increase of 130% with the inflow and 160% with the outflow. After that the difference decreases substantially. 0.5m to 0.25 inflows increase by 120% and the outflows 130%. After that the only notable difference is between 5 meter and 2.5 meters, in this case the outflow only decreases with 5%.

4.2.4 Temperatures

The temperature gradient between the u-pipe and borehole causes conduction of heat. This temperature gradient is especially important at the heating and cooling boundary, where it is the largest. Therefore, these temperatures have been alternated and their efficiencies have been compared. At first, only the temperature of the hot water for heating was varied. Secondly, the temperature of the cold water for cooling was varied. Lastly, the entire operation range, so the heating and cooling temperature, were either heightened or lowered and their influences looked at. for single cycle, in figure 21, it can be observed that the efficiency decreases as one increases the temperature of the heating water in the borehole. Initially in the transition from 50°C to 60°C there is not a substantial difference, the decrease in efficiency only becomes apparent at a heating temperature of 70°C.

4.2.4.1 Heating water temperature

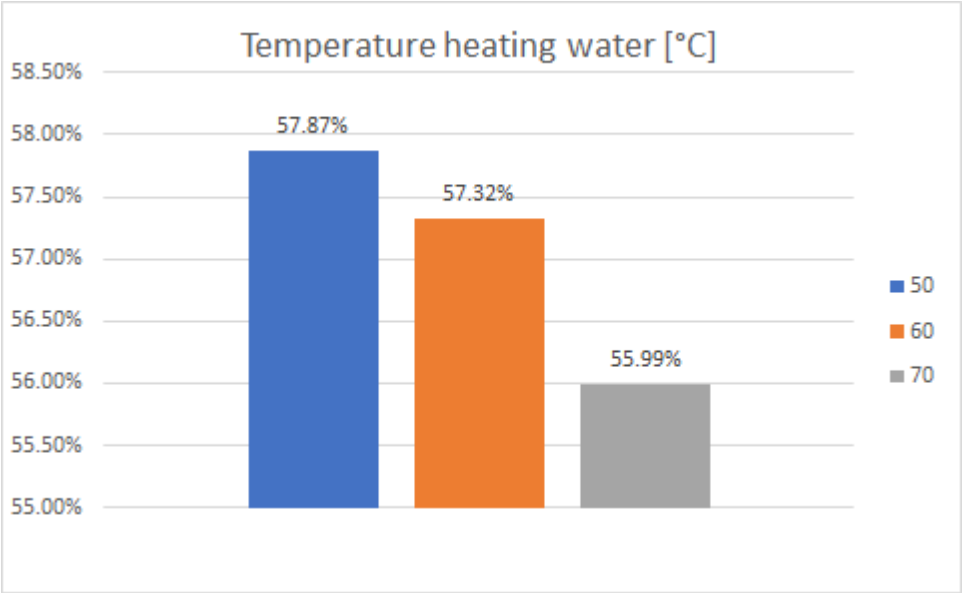

Figure 21: Comparison of the efficicency at varying Th; 1 cycle.

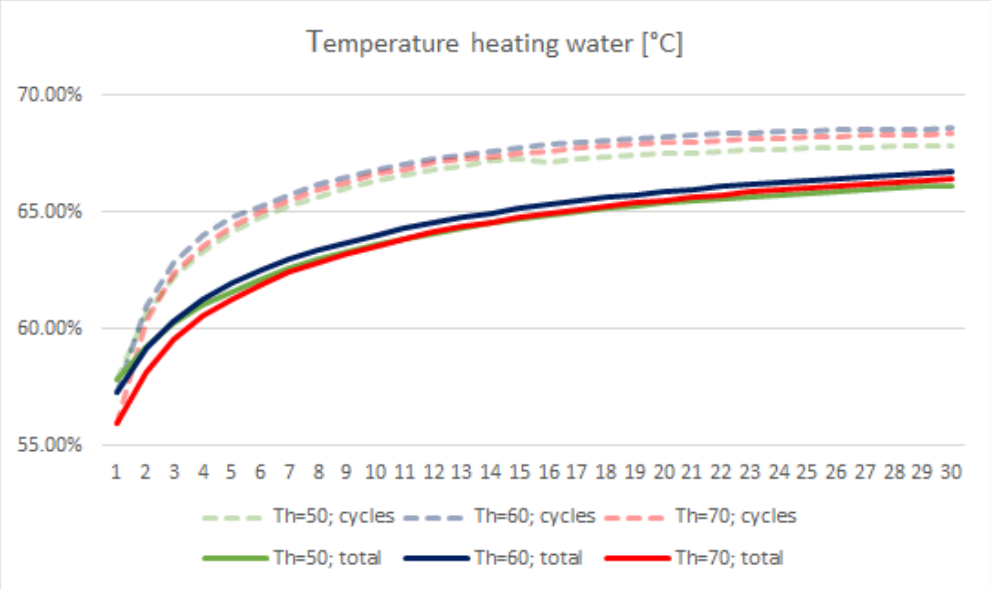

Figure 22: Comparison of the efficiency at varying Th; 30 cycle.

Thirty cycles

Figure 18 portrays that in hotter boreholes the accumulative efficiency takes longer to equate to the cycle efficiency. An interesting observation is that 60 degrees Celsius borehole is the most efficient. However, the 70 degrees Celsius borehole after 30 cycles is still suggesting further growth in efficiency.

Heat flow

The 70°C borehole in relation to the 60°C borehole has obtained greater heat flows. An increase of 120% for both in and out flows were recorded. From 50°C to 60°C the heat flow in and out increased with a percentage difference of 130%.

4.2.4.2 Cooling water temperature

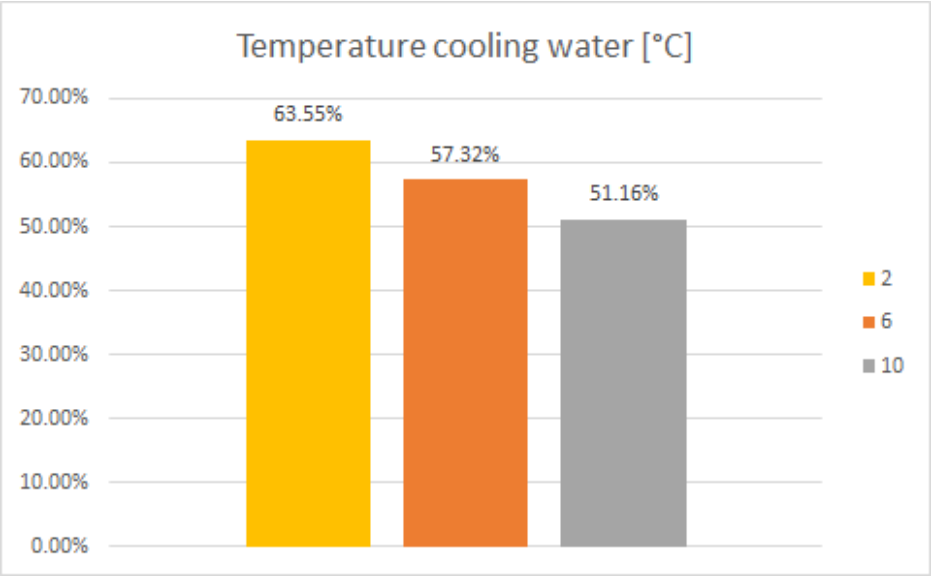

Figure 23: Comparison of the efficiency at varying Tc; 1 cycle.

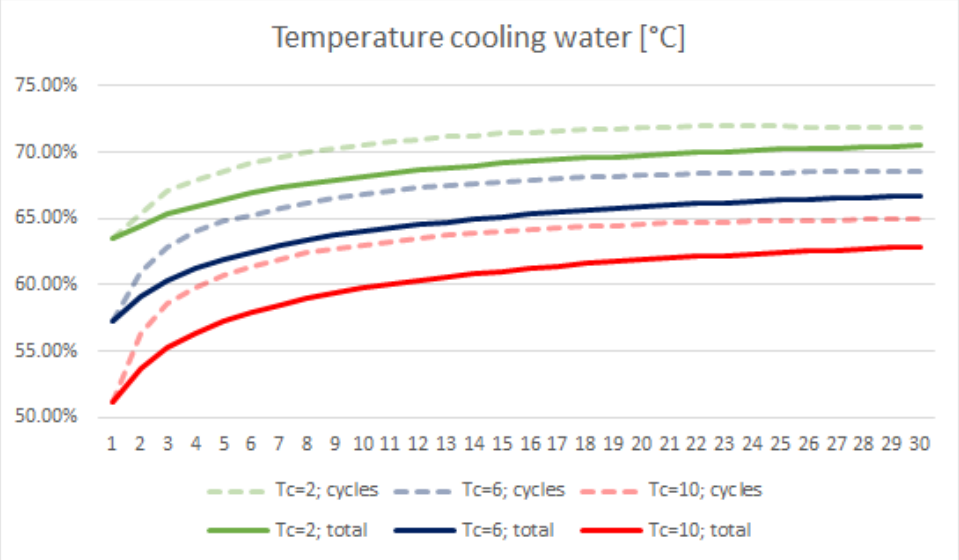

Figure 24: Comparison of the efficiency at varying Th; 30 cycles.

Single cycle

Figure 19 depicts that colder water has a higher efficiency than the relative warmer water. This is a logical result as colder water can absorb larger amounts of heat than warmer water.

Thirty cycles

In figure 20 the emphasis is made that the colder water is more efficient. What also can be seen is that the difference between the accumulated efficiency and the efficiency per cycle is increased throughout as the run progresses. The growth rate of efficiencies for the heating trajectory is significantly larger than the growth rate for cooling trajectory which is a notable difference.

Heat flow

Decreasing the cooling temperature of the cooling water from 10 °C to 6°C causes an increase of 2% and 8 % for the inflow and the outflow respectively. Changing the cooling water temperature from 6°C to 2°C increases the inflow with 2% and the outflow with 7%.

4.2.4.2 Operating temperature

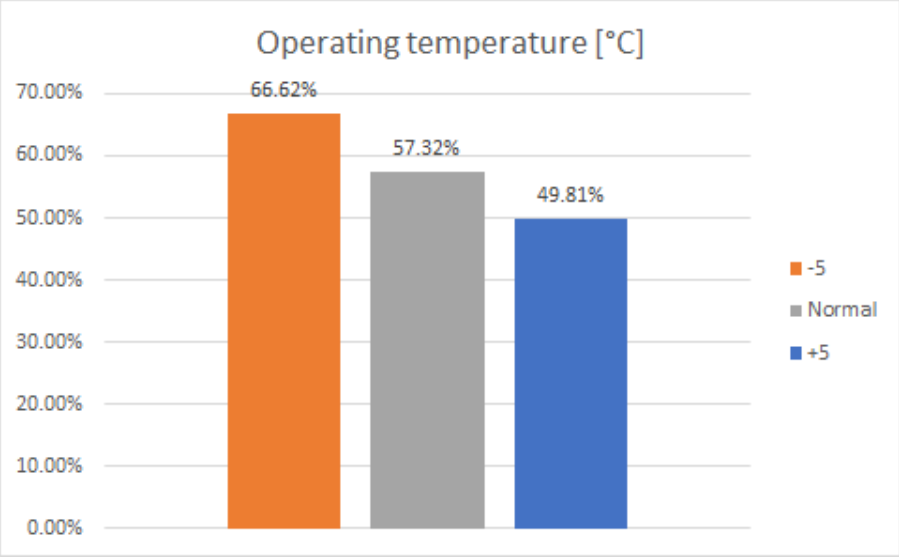

Figure 25: Comparison of the efficiency at varying operating temperature; 1 cycle.

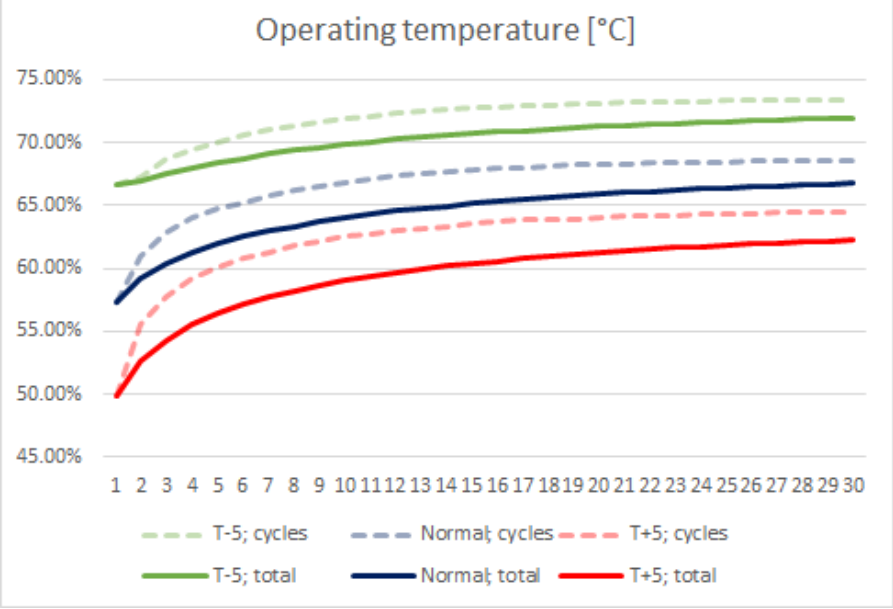

Figure 26: Comparison of the efficiency at varying operating temperature; 30 cycles.

Single cycle

Figure 21 shows a steady decrease in efficiency when the operating temperature is increased from -5°C to +5°C. This suggests that lower operating temperatures are beneficial for efficient boreholes.

Thirty cycles

In figure 22, it seems when both temperatures are heightened or lowered, the efficiency change can be mainly attributed to the change in the temperature of the cooling water, because there is a large difference which is not present when the heating water is hotter. A notable observation to changing the cooling water is that in the colder operating cycles the accumulated efficiency is much closer to the per cycle efficiency. Therefore, it can be stated that the driving force of the efficiency of borehole is the cooling water.

Heat flow

The contrast in heat flow between the 5 degrees Celsius operating temperature borehole and the 0 degrees Celsius operating temperature borehole is 10% larger inflow and 2% larger outflow.

The operational Temperature +5°C degrees to 0 yield 10% extra inflow and 2% extra outflow. A change from +0°C to -5°C gives an increase of 11% more inflow and 3 % more outflow.

5. Discussion

Looking at the results in the previous chapter some conclusions can be drawn, and possible explanations can be theorised. Some general outcomes will be described and after that some variable dependent phenomenon will be described.

5.1 Difference accumulated efficiency and per cycle efficiency

The accumulated efficiency always moves towards the efficiency per cycle, while the efficiency per cycle grows towards a limit. Here the efficiency per cycle starts of by increasing very fast but slowing down gradually towards a limit of the efficiency. While the accumulated efficiency starts of slower but increases more gradually to limit. This is explained by the accumulated efficiency being a result of all cycles and the efficiencies of the first cycles are always relatively low, so it takes a few cycles to decrease the effect of these cycles.

5.2 The duration of the efficiency to reach its limit

In both the case of the accumulated and per cycle efficiency it takes around 15 years before the logarithmic growth of the efficiency start to slow down. This behaviour is observed in all simulations. A noteworthy phenomenon is that the largest dispersions for this effect occur when varying the radius of the borehole and the temperature of the cooling water. A possible explanation for this 15-year duration originates from the radius. When one increases the radius, the time required for the borehole to reach a “steady state” also increases, this suggests that it has to do with the amount of energy in the borehole. A PCM holds more energy so takes more time to cool off. This hypothesis is also supported by the fact that similar behaviour is observed when using colder cooling water. As an increase in radius and a larger temperature difference would both cause the amount of possible energy extracted from the borehole to increase.

5.3 Optimal radius

There seems to be an optimum for the thickness of the PCM around the 0.5 to 1 meter radius. A possible explanation is that it occurs due to the principle that a material in its phase change trajectory does so at near constant temperature. This would mean that the PCM acts as a thermal isolator for the next step while phase changing. If this is the case if one were to make the radius too big, the PCM would not allow enough heat through on the cycle time scale used in this paper. Thus, a BTES system with a large PCM radius cannot access its entire thermal capacity due to the relatively low thermal diffusivity of the PCM when compared to soil.

5.4 Increasing the temperature of the heating water increases the capacity

By increasing the temperature of the water used to heat the borehole, the borehole absorbs and “discharges” more energy. This increases the usable thermal capacity of a borehole without losing much of the efficiency or having to increase the borehole in size. This can be explained by the fact that the heat flow is a result of a temperature gradient. Thus, by increasing the temperature of the heating water, the temperature gradient with the ground is increased, which results in a higher heat flow. Afterwards the borehole also has a higher temperature, so the same effect works the other way around too and more energy is also recovered.

6. Conclusion

The main question of this research is: *In what ways does the energy performance of a phase change material (PCM) in a borehole process, confined to the Dutch mainland, change when varying the PCM, the mole fraction of the PCM, the diameter of the borehole or the temperature of heating and/or cooling?* First the best choice for a PCM will be discussed, which is followed by the mole fraction, the radius and the temperature range.

The results show that using a PCM increases the energy performance of a borehole compared to only using sand such as in a traditional borehole. Using sand yielded an efficiency of the borehole of 29% in the first year and an accumulated average of approximately 34% over 30 years and cycles. The PCM RT35Hc gave a first-year efficiency of 57.32% and approached a value of around 62% over 30 years. The energy performance of the PCM RT44Hc is 54.90% in the first year and reaches approximately 59% in a 30-year period. It can thus be concluded that using the PCM RT35Hc yields the highest energy performance.

As expected, the efficiency increases as the mole fraction becomes larger. Thereby, from figure 14 it can be concluded that using PCM makes an enormous difference in comparison to solely sand. Increasing the mole fraction of PCM causes a logarithmically scaled increase in the energy efficiency. The efficiency increases from 29.53% for pure sand up to 57.32% for pure PCM.

The radius seems to have an optimum of around 1 meter PCM where the energy performance equals 66.73%. While the efficiency steadily increases when the radius is increased up to 1 meter, further increasing the radius gives rise to a fall in energy performance. The accumulated efficiencies of the PCM are 47.77%, 59.88%, 66.22%, 66.73%, 65.35% and 61.97% for a length of 01; 0.25; 0.5; 1; 2.5 and 5 m respectively.

Changing the heating temperature does not seem to have a large impact, at best increasing the energy performance from 66.15% to 66.41% while the cooling temperature makes the borehole much more efficient, from 66.41% to 70.48%. Lastly, when changing both the heating and cooling temperatures, the cooling temperature's effect is dominant. When combining the effects of both cooling water and heating water one gets the highest energy performance of 71.93%.

7. Evaluation

Various points should be evaluated. A list of the discussion points is found below. Those are the compromises made in order to save runtime, the effects of numerical dispersion and the fact that the heating and cooling temperature is kept constant over the depth of the borehole.

7.1 Compromising t_{end} or L_{tot} in order to save runtime

The total running time (t_{end}) was chosen as an entire year at first, so 31,536,000 seconds. This allowed for a yearly cycle of heating during the spring and summer and cooling between the autumn and winter. This already showed some severe differences in efficiencies between different PCM's and concentrations. Based upon these clear differences it was decided not to run those simulations again for our lifetime estimate of 30 years. If this would have been done, slightly different efficiencies might have arisen, even though the difference is as big that the favourability of for example a mole fraction of 1 would still overshadow the mole fraction of 0.8. Therefore, it was chosen not to run those simulations again for thirty cycles. This can of course still be done in the future; might the need to do so arise. For simulations that did not have a result that was that clear yet, it was decided to run those for a total of 30 years (946,080,000 seconds), as 30 years is a lifetime estimate of most BTES projects. A decreasing efficiency due to wear of the borehole was neglected, as well as the fact that after 30 years a borehole can still be of use.

The final factor that has not been discussed yet, that severely influences the running time is the total radius considered (L_{tot}). The last element in the radius in the numerical model is calculated using the ground temperature, which remains constant, even though over the duration of several years a slow but steady rise is expected. This problem is addressed by increasing the radius of the model to such a degree that it reaches the steady-state conditions for a borehole consisting out of solely sand. During the single cycle runs, the L_{tot} = 20 m was used. During the longer runs L_{tot} = 40 m was used as the heat has more time to reach the end of the model.

Furthermore, the research would have been more accurate if dt and dL were smaller and L_{tot} was larger. Unfortunately, the computers used to run the numerical model approached their limit in RAM memory, so a higher accuracy was not possible. Obviously, this problem could have been solved by running the numerical model in batches, which was not considered as necessary.

7.2 Numerical dispersion

One effect that was noted during the testing of the numerical model was that changing the length step affected the results. While it is expected that increasing the amount of grid points would increase the accuracy of results, it is not expected that the result varies significantly. three separate causes were identified as possible causes for this unexpected step length dependency.

7.2.1 Volume estimate inaccuracy

The first possible cause is the assumption made in the derivation of equation 15, the governing equation of the model. The formula for the volume of the circle element was simplified on the basis that the distance to point i was the dominant factor. As both the correct and simplified formulas for the volume are known it is possible to calculate how large the error within the model is. Using the model's values for the u-pipe radius and step length the volume error can be calculated. Table 3 gives some select values of the volume error and shows that while the initial mistake is significant, it rapidly shrinks in effect. Considering the model has 800 length steps in its current configuration and the volume error is only significant in the first couple of steps of the model this problem was deemed of negligible consequence to the reliability of the results.

Table 6: Volume approximate over volume.

Step number [#]	Volume approximate over volume
1	80.00 %
10	96.00 %
50	99.05 %
100	99.51 %

7.2.2 Effect surface area heat inflow

The initial inlet of heat takes place at the boundary of the pipe with hot (or during the cooling phase cold) water. The area of this heat inflow should be calculated according to the formula $2\pi\ r\ l$. The model overshoots this area with a factor *½dL* as the radius for heat transfer is calculated as R_{cen}+*½dL*, as this is the first border between the point where the upper boundary is valid and where the point where the first actual temperature is calculated. Realising that this happens for every simulation, the comparison remains valid.

7.2.3 Speed heat dispersion

Each timestep the temperature in a certain element is based upon the temperature in the neighbouring elements in the previous timestep. This allows for a faster heat transfer when the length step is larger, as the heat can only transfer 1 *dL* further each timestep. This is illustrated in figure 23. Especially when using a PCM of great length (such as 2.5 or 5m), this phenomenon of thermal inertia is a very likely explanation for the lower efficiency results.

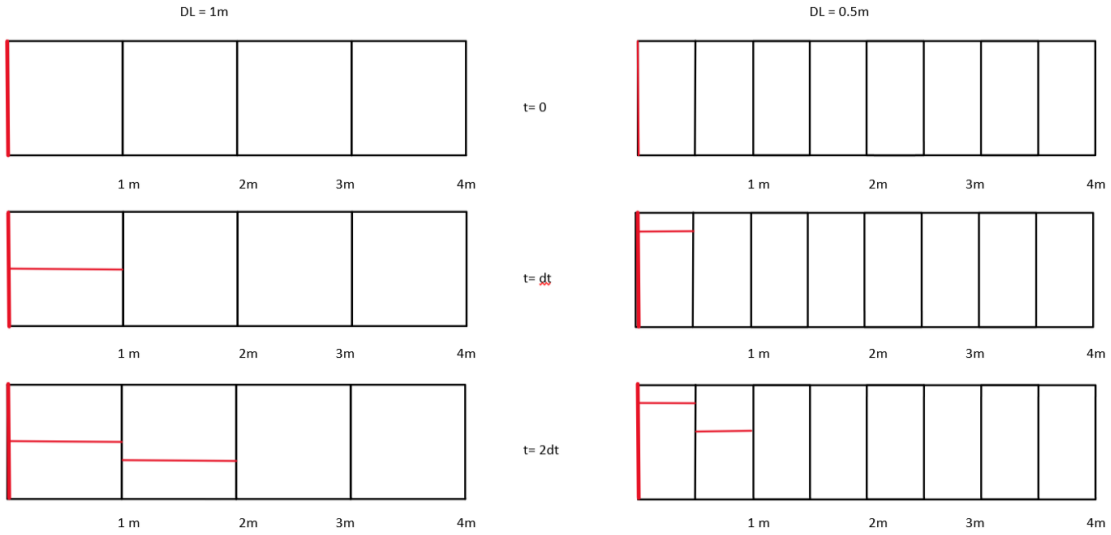

Figure 27: Heat transfer in timesteps.

7.3 Temperature of the water constant over the depth of the borehole

The assumption that the temperature of the water used for the heating and the cooling of the borehole is constant was made to keep the model viable for a 1D-analysis. This is not the case in an actual borehole. The water for heating does decrease as the water goes deeper into the borehole. So in actuality less heat would be transferred at greater depth. When being cooled again, the water flowing through the borehole will heat up, so that at greater depth also less heat is extracted due to a smaller gradient.

When utilizing the fact that the water changes temperature over depth, a 2D-analysis improve the numerical method, which would mean increasing the calculation time of the model in two ways. Firstly, it would add a dimension. Secondly, vertical heat flow would also have to be considered, increasing the number of calculations for the temperature of a certain grid point.

8. Recommendations

Noting the results captured in this report, further research can be done into the subject of PCM boreholes. Diverse options are explained below.

A 2D analysis would expand the scope of effects that can be simulated in a numerical model. Specifically, such a model would be able to simulate the effects of different soils at different heights.

An economic model could be made to test the economic viability of the PCM borehole. This is especially interesting when comparing a 0.5m PCM borehole with a 1.0m PCM borehole to investigate whether the increase in capital costs for the larger PCM radius will make up in efficiency over the years.

Other locations could be tested, other than the Dutch mainland. Therefore, other soil conditions must be considered. Expanding the scope to investigate if specific geographical regions are suited for this technology would provide valuable insight into which regions would profit from pursuing this technology.

Furthermore, constructing a physical prototype would enable researchers to investigate if any physical or chemical processes would present themselves in borehole operation. As the numerical model solely investigates the BTES system as an energy system such effect would not be represented in the results.

The effect of groundwater to a PCM boreholes could be researched. Whether this gives rise to more heat loss and thus a lower efficiency, is yet to be illustrated. In addition,

The effect that boreholes have on each other could cause changes, specifically the trade-off of thermal capacity and isolation that is gained/lost by building a borehole close to another borehole.

Bibliography

BTES | Underground Energy. (2019). Applied Hydrogeology Geothermal Innovation. https://underground-energy.com/our-technology/btes/

Huang, S., Ma, Z., & Cooper, P. (2014). Optimal design of vertical ground heat exchangers by using entropy generation minimization method and genetic algorithms. Energy Conversion and Management, 87, 128–137. https://doi.org/10.1016/j.enconman.2014.06.094

Indra Noer Hamdhan and Barry G. Clarke. Bandung National of Institute of Technology, Leeds University. (2010 april 25). Determination of Thermal Conductivity of Coarse and Fine Sand Soils. Geraadpleegd op 24 september. https://www.geothermal-energy.org/pdf/IGAstandard/WGC/2010/2952.pdf

Jaime van Trikt & Hansjorg Ahrens, Naturalis. Geologie van nederland. https://www.geologievannederland.nl/ondergrond/bodems . Consulted on 23 september 2020

Lanini, S., Delaleux, F., Py, X., R.Olivès, & Nguyen, D. (2014). Improvement of borehole thermal energy storage design based on experimental and modelling results. Energy and Buildings, 77, 393–400. https://doi.org/10.1016/j.enbuild.2014.03.056

Nakevska, N., Schincariol, R. A., Dehkordi, S. E., & Cheadle, B. A. (2014). Geothermal Waste Heat Utilization from In Situ Thermal Bitumen Recovery Operations. Groundwater, 53(2), 251–260. https://doi.org/10.1111/gwat.12196

Pasupathy, A., & Velraj, R. (2008, 1 januari). Phase change material-based building architecture for thermal management in residential and commercial establishments. Consulted on 20 september 2020, van https://www.sciencedirect.com/science/article/abs/pii/S1364032106000724

Prigogine, I., Defay, R. (1950/1954). Chemical Thermodynamics, Longmans, Green & Co, London, pages 22-23.

Rogelj, Joeri, et al. “Paris Agreement Climate Proposals Need a Boost to Keep Warming Well below 2 °C.” Nature, vol. 534, no. 7609, 2016, pp. 631–39. Crossref, doi:10.1038/nature18307.

Rubitherm. (2020, October 9). Rubitherm.Eu.
https://www.rubitherm.eu/media/products/datasheets/Techdata_-RT44HC_EN_09102020.PDF
https://www.rubitherm.eu/media/products/datasheets/Techdata_-RT35HC_EN_09102020.PDF

Shapiro, M. A. (2020). Principles of Engineering Thermodynamics (8th Edition). W.

Skarphagen, H., Banks, D., Frengstad, B. S., & Gether, H. (2019). Design Considerations for Borehole Thermal Energy Storage (BTES): A Review with Emphasis on Convective Heat Transfer. Geofluids, 2019, 1–26. https://doi.org/10.1155/2019/4961781

Stene, J. (19 May 2008), "Large-Scale Ground-Source Heat Pump Systems in Norway" (PDF), Large-Scale Ground-Source Heat Pump Systems in Norway, IEA Heat Pump Annex 29 Workshop, Zurich

Stichting Deltawerken Online. (2004). Geology of the Netherlands. Consulted on 23 september 2020. Van http://www.deltawerken.com/Geology-of-the-Netherlands/112.html.

Stuart Kenneth Haigh. (2012 July). Thermal conductivity of sand. Consulted on 24 september 2020.

https://www.researchgate.net/publication/274765037_Thermal_conductivity_of_sands

Welsch, B., Rühaak, W., Schulte, D. O., Bär, K., & Sass, I. (2016). Characteristics of medium deep borehole thermal energy storage. International Journal of Energy Research, 40(13), 1855–1868. https://doi.org/10.1002/er.3570

Zhang, C., Hu, S., Liu, Y., & Wang, Q. (2016). Optimal design of borehole heat exchangers based on hourly load simulation. Energy, 116, 1180–1190. https://doi.org/10.1016/j.energy.2016.10.045

Appendix 1: Python code

```python
import pandas as pd
import numpy as np
import matplotlib.pyplot as plt


"Initial values"
"Temperature"
Tw1 = 60 + 273 #Temperature hot water [K]
Tw2 = 6 + 273 #Temperature cold water [K]
Teind = 12 + 273 #Temperature ground [K]
"Length"
Rcen = 0.1 #Radius heating/cooling pipe [m]
Lpcm = 1  #Length PCM [m]
Lzand = 39 #Length of Sand from PCM to end of model [m]
dL = 0.05 #Length step [m]
h = 10 #height of the borehole [m]

"Time"
t0 = 0 #Initial time [s]
tl = 3600*24*365*30 #End time [s]
dt = 120 #Timestep [s]
cycles = 30 #Amount of cycles

"Material properties"
"PCM"
naam = "pcm rt35hc"
rhos = 880
rhol = 770
kappa1 = 0.2
Ts = 34+273 #initial temperature smelt solid
Tl = 36+273 #final temperature smelt solid
Cppcm = 2000
latentheat = 240000-2000 #heatstorage - sensibleheat
"Sand"
rho2 = 1631
kappa2 = 2
Cp2 = 1200

"Mix"
mix = 1 #Molfraction PCM
Cp1 = Cppcm * mix + Cp2 * (1-mix)


def cp(T): #To look at slope discontinuity in graph for PCM
    if Ts < T < Tl:
        CP = Cp1 + latentheat*mix
    else:
        CP = Cp1
    return CP

def rho(T):
    if T<=Ts:
        RHO = rhos
    else:
        RHO = rhol
    return RHO

```

```
def alfa(T,L):
    if  L <= Lpcm:
        X = kappa1/(rho(T)*cp(T))
    elif Lpcm < L:
        X = kappa2/(rho2*Cp2)
    return X

def Temp(T0,T1,T2,L):
    R = L+ Rcen
    Tn = T1 + dt*(((T0 -T1)*(2*R-dL)+(T2-T1)*(2*R+dL))/(dL**
                2))*alfa(T1,L)/(2*R)
    return Tn

def heatflow(T0, T1):
    R = Rcen
    Q = 2*np.pi*h*(R+0.5*dL)*kappa1*((T0-T1)/dL) *dt #Q=A*k*DT/DX
    return Q

def jurriaan(T0, T1):
    R = Rcen
    q = 2*np.pi*h*kappa1*((T0-T1)/dL)*(2*R+dL)/(2*R) *dt  #Q=A*k*DT/DX
    return q
```

```
def intern(T,tijd,leng):
    Uin = 0
    Uover = 0
    for n in range(len(T[int(len(tijd)/2-1)])):
        if n == 0 :
            continue
        elif leng[n] <= Lpcm:
            if T[int(len(tijd)/2-1),n]<Ts  :
                Uin = Uin + (T[int(len(tijd)/2),n]-Teind)* Cppcm*rhos*(2*np.pi*
                          (leng[n]+Rcen)*dL*h)
            elif Ts <= T[int(len(tijd)/2),n]< Tl:
                Uin = Uin + ((Ts-Teind)*Cppcm*rhos + (T[int(len(tijd)/2),n]
                -Ts)*(latentheat+Cppcm)*rhol)*(2*np.pi*(leng[n]+Rcen)*dL*h)
            else:
                Uin = Uin + ((Ts-Teind)*Cppcm*rhos + (Tl-Ts)*(latentheat
                           +Cppcm)*rhol+ (T[int(len(tijd)/2),n]-Tl)*Cppcm
                    *rhol)*(2*np.pi*(leng[n]+Rcen)*dL*h)
        elif Lpcm < leng[n]:
            Uin = Uin + (T[int(len(tijd)/2),n]-Teind)*rho2*Cp2*(2*np.pi
                        *(leng[n]+Rcen)*dL*h)

    for n in range(len(T[-1])):
        if n == 0 :
            continue
        elif leng[n] <= Lpcm:
            if T[-1,n]<Ts  :
                Uover = Uover + (T[-1,n]-Teind)* Cppcm*rhos*(2*np.pi*(leng[n]
                +Rcen)*dL*h)
            elif Ts<T[-1,n]< Tl:
                Uover = Uover + ((Ts-Teind)*Cppcm*rhos + (T[-1,n]
                -Ts)*(latentheat+Cppcm)*rhol)*(2*np.pi*(leng[n]+Rcen)*dL*h)
            else:
                Uover = Uover + ((Ts-Teind)*Cppcm*rhos + (Tl-Ts)*(latentheat
                                 +Cppcm)*rhol+ (T[-1,n]-Tl)*Cppcm*rhol)*(2
                    *np.pi*(leng[n]+Rcen)*dL*h)
        elif Lpcm < leng[n]:
            Uover = Uover + (T[-1,n]-Teind)*rho2*Cp2*(2*np.pi*(leng[n]
            +Rcen)*dL*h)
    Uuit = Uin-Uover
    E = Uuit/Uin
    return E , Uin, Uuit, Uover
```

```
def time(t0,t1):
    N = int(np.round((t1-t0)/dt))+1
    time = np.linspace(t0,t1,num=N)
    I = int(np.round((LT)/dL))+1
    lengten = np.linspace(0,LT,num=I)
    T = np.full((time.size, lengten.size),Teind+0.0)
    T[:,0] = Tw1
    hf = np.zeros(time.size) #heatflow
    U = np.zeros(time.size)
    V = np.zeros(lengten.size-1)
    jhf = np.zeros(time.size)
    for n in range(len(U)):
        if n == 0:
            continue
        elif n/(N/cycles)-int(n/(N/cycles)) >= 1/2:
            T[n,0] = Tw2
        for i in range(len(V)):
            if i == 0:
                continue
            T[n,i] = Temp(T[n-1,i-1],T[n-1,i],T[n-1,i+1],lengten[i])
        T[n,-1] = Temp(T[n-1,-2],T[n-1,-1],Teind,LT)
        hf[n] = heatflow(T[n-1,0],T[n-1,1])
        jhf[n] =  jurriaan(T[n-1,0],T[n-1,1])

    T[-1,0] = Tw2
    T[-1,-1] = Temp(T[-2,-2],T[-2,-1],Teind,LT)
    hf[-1] = heatflow(T[-2,0],T[-2,1])
    jhf[-1] = jurriaan(T[-2,0],T[-2,1])
    return lengten, time, T, hf, jhf

def eta(Q):
    Qin = 0
    Quit = 0
    for n in range(len(Q)):
        if Q[n] <= 0:
            Quit = Quit + abs(Q[n])
        else:
            Qin = Qin + Q[n]
    Eperformance = Quit/Qin
    return Eperformance


def Qinuit(Q):
    Qin = 0
    Quit = 0
    for n in range(len(Q)):
        if Q[n] <= 0:
            Quit = Quit + abs(Q[n])
        else:
            Qin = Qin + Q[n]
    return Qin , Quit

def plot(tijd,L,T,n):
    plt.plot(L+Rcen,T ,linestyle='-',label= round(n/3600/24)) #days
    plt.xlabel('$L$')
    plt.ylabel('$T(L)$')
    plt.legend()
    return
```

```
181
182 plt.close('all')
183 LT = Lpcm + Lzand
184 leng, tijd, T, hf ,jhf= time(t0,t1)
185 uren = t1/3600
186 dagen = uren/24
187 weken = dagen/7
188 jaren = weken/52
189
190
191 PA = cycles*10+1 #number of plots
192 Deler = PA-1
193 for n in range(PA):
194     if n == 0:
195         continue
196     elif (n-1)/10 - int((n-1)/10) == 0:
197         plt.figure("cycle "+ str(int((n-1)/10)+1))
198     plot(tijd[int(n*len(tijd)/Deler-1)],leng, T[int(n*len(tijd)/Deler
199                   -1),:], n*(len(tijd)-1)*dt/Deler)
200     plt.savefig("cycle "+ str(int((n-1)/10)+1))
201
202 cyc = np.array_split(hf,cycles)
203 performances = np.zeros([2,cycles])
204 legenda = []
205 added =np.array([])
206 for i in range(cycles):
207     performances[0,i] = eta(cyc[i])
208     legenda.append("efficienty cycle "+ str(i+1))
209     added = np.append(added, cyc[i])
210     performances[1,i] = eta(added)
211
212
213 Eff3 = eta(jhf)
214 Qin3, Quit3 = Qinuit(jhf)
215
216 print(performances)
217 print(legenda)
218 print("total efficiency 1 = ", eta(hf))
219 Qin, Quit = Qinuit(hf)
220 print("heat flow in = ", Qin,"heat flow uit = ",Quit)
221
222
```

```
223 waardes = ('Temperatuur \nhete water {}K, koud water {}K'+
224            'en grondtemperatuur {}K'+
225            '\nlengtes \nwaterbuislengte {}m, PCMlengte {}m, zandlengte {}m'+
226            'DL {}m en hoogte {}m '+
227            '\ntijd \neindtijd {} dagen, tijdstap {}s en cycles {}'+
228            '\nmateriaal \nPCM {} en molfractie PCM {}')
229 filename2 = 'data t={}h {} mengsel{} straal{} performance.txt.'
230 with open(filename2.format(uren,naam, 1-mix,Lpcm ),'w') as f:
231     f.write(waardes.format(Tw1,Tw2,Teind,Rcen, Lpcm, Lzand, dL, h, t1/3600/24,
232                            dt, cycles,naam,mix)
233             +"\n----------------------------- "
234             +"\n performance met warmtestromen is \n"
235             + str(performances)
236             + "\n in volgorde \n"
237             + str(legenda)
238             + "\n heatflow in "
239             + str(Qin)
240             + "\n heatflow uit "
241             + str(Quit)
242             +"\n---------------------------- "
243             +"\n performance met Dl factor en warmtestroom "
244             + str(Eff3)
245             + "\n heatflow in "
246             + str(Qin3)
247             + "\n heatflow uit "
248             + str(Quit3)
249             )
250     f.close()
251
252 print("----------------\nefficienty 3 = ",Eff3)
253 print("warmtestroom 3 = ",[Qin3,Quit3])
```

Appendix 2: Table of results simulations

A: Results 1 cycle

Number	PCM	L_{total}	Radius [m]	Molfraction [m%]	Cycles [-]	T_h [°C]	T_c [°C]	Efficiency [%]	Q_{in} [J]	Q_{uit} [J]
1	Sand	20	0	1	1	60	6	29.53%	2611102792	771117812.3
2	RT35hc	20	1	1	1	60	6	57.32%	4614621529	2644940166
3	RT44hc	20	1	1	1	60	6	54.90%	4262789880	2340123922
4	RT35hc	20	0.1	1	1	60	6	39.03%	3016681302	1177467204
5	RT35hc	20	0.25	1	1	60	6	52.18%	3876681394	2022735944
6	RT35hc	20	0.5	1	1	60	6	57.99%	4458423045	2585258247
7	RT35hc	20	2.5	1	1	60	6	49.42%	4700794885	2323145645
8	RT35hc	20	5	1	1	60	6	48.28%	4701529589	2269961626
9	RT35hc	20	1	0.2	1	60	6	47.48%	3593952469	1706424892
10	RT35hc	20	1	0.4	1	60	6	51.47%	3931740658	2023767055
11	RT35hc	20	1	0.6	1	60	6	54.00%	4197907442	2266730764
12	RT35hc	20	1	0.8	1	60	6	55.93%	4418996186	2471369333
13	RT35hc	40	1	1	30	60	6	66.73%	1.34029E+11	89441739476
14	RT35hc	20	1	1	1	50	6	57.87%	3436864470	1988759416
15	RT35hc	20	1	1	1	70	6	55.99%	5721533706	3203231762
16	RT35hc	20	1	1	1	60	10	51.16%	4614621529	2360983333
17	RT35hc	20	1	1	1	60	2	63.55%	4614621529	2932538798
18	RT35hc	20	1	1	1	65	11	49.81%	5175124595	2577662891
19	RT35hc	20	1	1	1	55	1	66.62%	40370959740	26894994498

B: Results thirty cycles

Number	PCM	L_{total}	Radius [m]	Molfraction [m%]	Cycles [-]	T_h [°C]	T_c [°C]	Efficiency [%]	Q_{in} [J]	Q_{uit} [J]
13	RT35hc	40	1	1	30	60	6	66.73%	1.34029E+11	89441739476
20	RT35hc	40	5	1	30	60	6	61.97%	1.34532E+11	83364949180
21	zand	40	0	1	30	60	6	38.98%	72428720751	28231199174
22	RT44hc	40	1	1	30	60	6	64.03%	1.23989E+11	79395390490

23	RT35hc	40	0.1	1	30	60	6	47.77%	84675425164	40447115785
24	RT35hc	40	0.25	1	30	60	6	59.88%	1.10394E+11	66099200521
25	RT35hc	40	0.5	1	30	60	6	66.22%	1.31277E+11	86928743144
26	RT35hc	40	2.5	1	30	60	6	65.35%	1.33105E+11	86988331538
27	RT35hc	40	1	1	30	50	6	66.15%	1.00506E+11	66481884948
28	RT35hc	40	1	1	30	70	6	66.41%	1.64696E+11	1.09378E+11
29	RT35hc	40	1	1	30	60	10	62.84%	1.31787E+11	82817630216
30	RT35hc	40	1	1	30	60	2	70.48%	1.36276E+11	96050117575
31	RT35hc	40	1	1	30	65	11	62.26%	1.46787E+11	91386636820
32	RT35hc	40	1	1	30	55	1	71.93%	1.20471E+11	86650593642

Appendix 3: Heat flow comparison

1 is the first mentioned situation and 2 is second mentioned situation.

	1		2		Difference 1-2		Percentage 1/2	
1-2	Qin	Quit	Qin	Quit	Qin	Quit	Qin	Quit
RT35hc-sand	1.34029E+11	89441739476	72428720751	28231199174	61599797112	61210540302	185.05%	316.82%
RT35hc - Rt44hc	1.34029E+11	89441739476	1.23989E+11	79395390490	10039272245	10046348986	108.10%	112.65%
Radius 0,25-0,1	1.10394E+11	66099200521	84675425164	40447115785	25718576343	-25652084736	130.37%	163.42%
Radius 0,5 - 0,25	1.31277E+11	86928743144	1.10394E+11	66099200521	20882501991	-20829542622	118.92%	131.51%
Radius 1 - 0,5	1.34029E+11	89441739476	1.31277E+11	86928743144	2752014365	-2512996332	102.10%	102.89%
Radius 2,5 - 1	1.33105E+11	86988331538	1.34029E+11	89441739476	-923100206.7	2453407938	99.31%	97.26%
Radius 5 - 2,5	1.34532E+11	83364949180	1.33105E+11	86988331538	1426268131	3623382358	101.07%	95.83%
Th 70 - 60	1.64696E+11	1.09378E+11	1.34029E+11	89441739476	30667368763	19936261736	122.88%	122.29%
Th 60 - 50	1.34029E+11	89441739476	1.00506E+11	66481884948	33522811320	22959854528	133.35%	134.54%
Tc 10 - 6	1.31787E+11	82817630216	1.34029E+11	89441739476	-2241348434	-6624109260	101.70%	108.00%
Tc 6 - 2	1.34029E+11	89441739476	1.36276E+11	96050117575	-2247268780	-6608378099	101.68%	107.39%
Top '+5' - 0	1.46787E+11	91386636820	1.34029E+11	89441739476	12758498329	1944897344	109.52%	102.17%
Top 0 - '-5'	1.34029E+11	89441739476	1.20471E+11	86650593642	13557583013	2791145834	111.25%	103.22%

Appendix 4: Deriving the stability condition using Fourier numbers

- Taking equation 11, opening up the brackets and taking the – of the alpha component into the equation gives us:

$$T_i^{n+1} = T_i^n + \frac{\propto \Delta t}{r} \frac{T_{i+1}^n\left(r+\frac{\Delta r}{2}\right) - T_i^n\left(r+\frac{\Delta r}{2}\right) + T_{i-1}^n\left(r-\frac{\Delta r}{2}\right) - T_i^n\left(r-\frac{\Delta r}{2}\right)}{\Delta r^2} \quad [20]$$

- Moving the Δr^2 component to the left and grouping for the relevant variable, T_i^n

$$T_i^{n+1} = T_i^n + \frac{\propto \Delta t}{r\,\Delta r^2}\left(-T_i^n\left(\left(r+\frac{\Delta r}{2}\right)+\left(r-\frac{\Delta r}{2}\right)\right) + T_{i+1}^n\left(r+\frac{\Delta r}{2}\right) + T_{i-1}^n\left(r-\frac{\Delta r}{2}\right)\right) \quad [21]$$

- Substituting the Fourier number into the equation and solving the coefficient of $-T_i^n$

$$T_i^{n+1} = T_i^n + \frac{Fo}{r}\left(-T_i^n(2r) + T_{i+1}^n\left(r+\frac{\Delta r}{2}\right) + T_{i-1}^n\left(r-\frac{\Delta r}{2}\right)\right) \quad [22]$$

$$\text{with; } Fo = \frac{\propto \Delta t}{\Delta r^2}$$

- Solving the outer most brackets and grouping for T_i^n:

$$T_i^{n+1} = (1 - 2\mathrm{Fo})\,T_i^n + Fo\,\frac{T_{i+1}^n\left(r+\frac{\Delta r}{2}\right) + T_{i-1}^n\left(r-\frac{\Delta r}{2}\right)}{r} \quad [23]$$

- Abiding by the condition that the coefficient of T_i^n cannot be negative this means that:

$$Fo \leq \frac{1}{2} \rightarrow \frac{\propto \Delta t}{\Delta r^2} \leq \frac{1}{2} \rightarrow \Delta t \leq \frac{\Delta r^2}{2 \propto} \quad [24]$$

Appendix 5: PCM datasheets

A: Data sheet for RT44hc

Data sheet

RUBITHERM

RT44HC

RUBITHERM® RT is a pure PCM, this heat storage material utilising the processes of phase change between solid and liquid (melting and congealing) to store and release large quantities of thermal energy at nearly constant temperature.
The RUBITHERM® phase change materials (PCM's) provide a very effective means for storing heat and cold, even when limited volumes and low differences in operating temperature are applicable.

Properties for RT-line:
- high thermal energy storage capacity
- heat storage and release take place at relatively constant temperatures
- no supercooling effect, chemically inert
- long life product, with stable performance through the phase change cycles
- melting temperature range between -9 °C and 100 °C available

The most important data:	Typical Values	
Melting area	41-44 main peak: 43	[°C]
Congealing area	44-40 main peak: 43	[°C]
Heat storage capacity ± 7,5% Combination of latent and sensible heat in a temperatur range of 35°C to 50°C.	250	[kJ/kg]*
	70	[Wh/kg]*
Specific heat capacity	2	[kJ/kg·K]
Density solid at 25°C	0,8	[kg/l]
Density liquid at 80°C	0,7	[kg/l]
Heat conductivity (both phases)	0,2	[W/(m·K)]
Volume expansion	12,5	[%]
Flash point	>180	[°C]
Max. operation temperature	70	[°C]

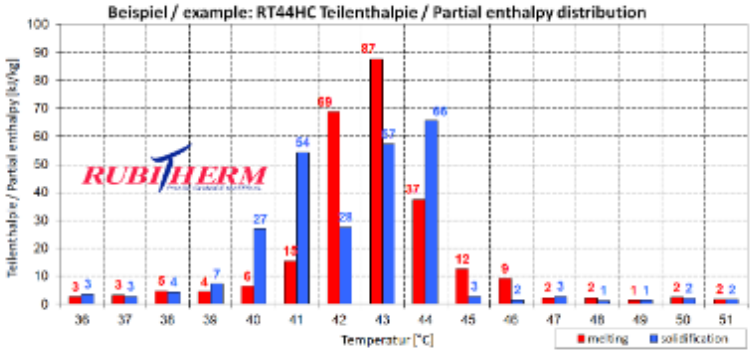

Rubitherm Technologies GmbH
Imhoffweg 6
D-12307 Berlin
phone: +49 (30) 7109622-0
E-Mail: info@rubitherm.com
Web: www.rubitherm.com

Version: 09.10.2020

(Rubitherm, *2020)*

B: Data sheet for RT35hc

Data sheet

RUBITHERM

RT35HC

RUBITHERM® RT is a pure PCM, this heat storage material utilising the processes of phase change between solid and liquid (melting and congealing) to store and release large quantities of thermal energy at nearly constant temperature.
The RUBITHERM® phase change materials (PCM's) provide a very effective means for storing heat and cold, even when limited volumes and low differences in operating temperature are applicable.

Properties for RT-line:
- high thermal energy storage capacity
- heat storage and release take place at relatively constant temperatures
- no supercooling effect, chemically inert
- long life product, with stable performance through the phase change cycles
- melting temperature range between -9 °C and 100 °C available

The most important data:	Typical Values	
Melting area	34-36 main peak: 35	[°C]
Congealing area	36-34 main peak: 35	[°C]
Heat storage capacity ± 7,5% Combination of latent and sensible heat in a temperatur range of 27°C to 42 °C.	240	[kJ/kg]*
	67	[Wh/kg]*
Specific heat capacity	2	[kJ/kg·K]
Density solid at 25°C	0,88	[kg/l]
Density liquid at 40°C	0,77	[kg/l]
Heat conductivity (both phases)	0,2	[W/(m·K)]
Volume expansion	12	[%]
Flash point	177	[°C]
Max. operation temperature	70	[°C]

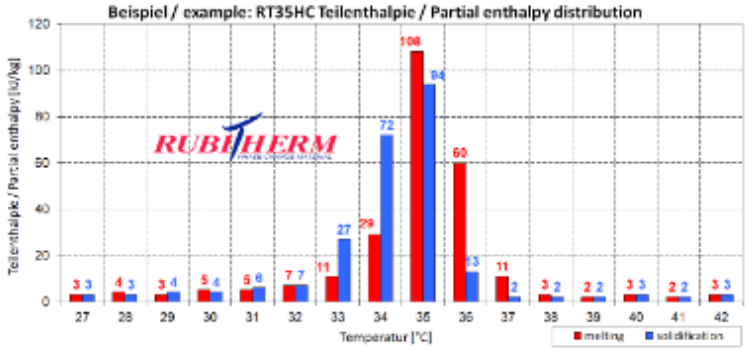

Rubitherm Technologies GmbH
Imhoffweg 6
D-12307 Berlin
phone: +49 (30) 7109622-0
E-Mail: info@rubitherm.com
Web: www.rubitherm.com

The product information given is a non-binding planning aid, subject to technical changes without notice.
Version: 09.10.2020

(Rubitherm, 2020)

Personal evaluation

Teise Stellema (4763165)

This project was a refreshing look upon heat transfer and programming simultaneously. The freedom my group members and I had concerning the approach for our project was very motivating and aided my critical and independent thinking. I strongly recommend this learning environment for future endeavours. Some aspects of the project were quite challenging and I therefore think it would be beneficial for new students to be supplied with more specific knowledge on the topics of heat transfer. I myself have a chemical engineering background and therefore heat transfer isn't new, however I do think this topic is taught in different ways at different faculties, so a more general and fundamental introduction into the underlying engineering aspect would be helpful. Overall, I enjoyed this project and would like to thank my group members for being extremely helpful and hardworking.

Niels van Vliet (4952669)

Over the last couple of months, I have learned a lot about energy conversion and storage. Not only in this project, but in the entire minor. I would like to state that this project greatly improved my general impression of the minor. The topic was interesting and although a bit difficult at first, after the first week of Q2 it slowly started to sink in. I was a bit blindsided at the start of the minor by the fact that I did not follow any thermodynamic courses in my previous two years at the faculty of Civil Engineering.

I was very happy about the collaboration between the group members. Everyone was motivated and had a different skill set. Lucas was mainly the computer scientist behind Python, especially when the numerical model had to be developed. He was the one that initiated the first steps and put in the most work at first. After Q2 had started, I started to catch up and we worked on it together for several days. It was also decided at the start of Q2 that Lucas and I would work mostly on the model, and the others would start writing the report. Patrick mainly constructed the methodology and derived the analytical and numerical expressions. Also, his critical but constructive feedback as well as his presenting skills did not go unnoticed. Lars mainly worked on the report and especially I was happy that he was willing to do the entire layout of the report at the end twice! Teise was more of the chemical scientist in our group, especially at the start I got the feeling that he understood most of the material properties as his field of study is Molecular Sciences and Technology.

Furthermore, we as a group have certainly improved our communication skills. We started for another course in google docs, and Microsoft Teams certainly was an upgrade. Also, communication with our supervisors got better over the weeks. The PowerPoint slides we eventually started preparing certainly were helpful, not only for our supervisors, but also for clarifying our questions. I was also happy about our supervisors responding over questions asked via mail very quickly, often in 24 hours.

As a group we met many times over the last couple of months in Microsoft Teams and spend many hours working on the project. As we were most of the time not allowed to go the university, my group members were the only people I really know from my minor and over time we have sort of become digital friends, with its greatest highlight yet to come, the post-symposium drinks!

Patrick Widdows (4720318)

In order to evaluate my experience with the project wb3595 I think it of value to state my personal learning goals. For the entire minor as well as the project I aimed not to expand on my theoretical understanding of thermodynamics. Instead, I hoped to learn how I can take my theoretical knowledge and apply that to a practical problem. Essentially, how do I use what I know. In this I found the project entirely satisfying. Having to “translate” heat transfer equations to numerical models in order to simulate real-life behaviour was a wonderful experience in mediating the theoretics with the practical.
So regarding the case the project presented I am very pleased. The amount of guidance from the supervisors is a razor-thin line, I personally enjoyed the puzzling of it all but understand that as a multi-disciplinary minor you have to ensure accessibility. The supervisors themselves were quite wonderful. I greatly enjoy being able to learn from people that teach what they research. The only recommendation I have is that, when there are multiple supervisors, that they formulate their advice together before giving their recommendations/critiques. At times one supervisor would tell us to something one way and then the other would tell us this is wrong and to do it a different way. As some matters are just that of personal preference if they could agree beforehand it would prevent confusion.
I was quite happy with the project group, the multi-disciplinary nature made for a fun and realistic group dynamic. I was happy to experience that everyone was comfortable stating their preferred subject to work on and that everyone handled things professionally. Corona provided an additional communication challenge, this forced us to work more separately than we might have usually done. Even this provided a minor hurdle.

Lucas Wiedenhoff (4952332)

At the start of the project, I wasn’t sure if this would be interesting. But soon after starting reading into it with the literature study I found out that BTES is a very relevant technology which had lots of aspects one could play around with. I found it very interesting to think about which aspects changes its behaviour in which way. Because of this I understood heat transfer much better.

At the start, organizing things was a bit difficult because of the limited time we could meet physically. An aspect which I personally disliked. Because of this it was hard to grasp everyone's understanding of every aspect of the technology. Although these things became clearer as the project continued. It also helped that we got a presentation in the beginning of how a borehole could be implemented in a numerical model. This made making the code much easier and made subsequent edits to model more doable.

The fact that we had people from three kinds of studies gave the project a few different perspectives, while it also provided people with a role in the group. I found it also interesting to hear wat kind of things people had learned in different studies.

Lars Wielinga (4719670)

I experienced this project and minor as very educational, it lived up to expectations. Beforehand, I had never heard anything about BTES systems, but this project showed me this technology as very interesting. A plus is that much heat transfer theory of the minor subjects was reflected in the project, because of that the matter became extra clear to me. In the beginning, it was quite challenging where to start with the numerical model, but the lecture of Jurriaan was very helpful for some clarification, despite there were still enough uncertainties to explore. For me, the most interesting part was to find some unexpected results after the simulations.

The collaboration between all the group members was excellent. It was a nice experience to work together with several fields of study, with the advantage of dividing the tasks study-related. Overall I learned a lot last six months, partly because of the good help of the other group members and supervisors.